Ecological Modelling
August 2019, Volume 405 Pages 51-68
https://doi.org/10.1016/j.ecolmodel.2019.05.004
https://archimer.ifremer.fr/doc/00659/77124/

Implementation of an end-to-end model of the Gulf of Lions ecosystem (NW Mediterranean Sea). II. Investigating the effects of high trophic levels on nutrients and plankton dynamics and associated feedbacks

Diaz Frédéric [1, *], Banaru Daniela [1, *], Verley Philippe [2], Shin Yunne-Jai [3]

[1] Aix Marseille Univ, Univ Toulon, CNRS, IRD,MIO UM110, F-13288 Marseille, France.
[2] IRD, UMR 123 AMAP, TA40 PS2, Blvd Lironde, F-34398 Montpellier 5, France.
[3] Univ Montpellier, UMR 248 MARBEC, IRD, Bat 24 CC 093 Pl Eugene Bataillon, F-34095 Montpellier 5, France.

* Corresponding authors : Frédéric Diaz, email address : frederic.diaz@univ-amu.fr ; Daniela Banaru, email address : daniela.banaru@univ-amu.fr

Abstract :

The end-to-end OSMOSE-GoL model parameterized, calibrated and evaluated for the Gulf of Lions ecosystem (Northwestern Mediterranean Sea) has been used to investigate the effects of introducing two-ways coupling between the dynamics of Low and High Trophic Level groups.

The use of a fully dynamic two-ways coupling between the models of Low and High Trophic Levels organisms provided some insights in the functioning of the food web in the Gulf of Lions. On the whole microphytoplankton and mesozooplankton were found to be preyed upon by High Trophic Levels planktivorous groups at rates lower than 20% and 30% of their respective natural mortality rates, but these relatively low rates involved some important alterations in the infra-seasonal and annual cycles of both High and Low Trophic Levels groups. They induced significant changes in biomass, fisheries landings and food web interactions by cascading effects. Spatial differential impacts of High Trophic Levels predation on plankton are less clear except in areas in which primary productivity is high. Higher predation rates on plankton groups were encountered within the area of the Rhone river's influence and in areas associated to the presence of mesoscale eddies in the Northwestern part of the Gulf of Lions, especially. Generally, the pressure of the High Trophic Levels predation was the highest in areas of highest biomass whatever the plankton group considered.

The two-ways coupling between Low and High Trophic Levels models revealed both bottom-up and top-down controls in the ecosystem with effects on planktivorous species similar to those observed in the field. The use of the end-to-end model enabled to propose a set of potential mechanisms that may explain the observed decrease in small pelagic catches by the French Mediterranean artisanal fisheries over the last decade.

Highlights

► The two-ways coupling induced changes in biomass, landings and trophic interactions. ► The two-ways coupling changed infra-seasonal and annual cycles of the modeled high and low trophic levels. ► Bottom-up and top-down feedbacks occurred with wide effects on planktivorous species.

Keywords : End-to-end model, Two-ways coupling, Plankton, Fisheries, Food web functioning

1. Introduction

Human activities interacting with climatic variability related to both natural and anthropogenic sources induce major changes in marine ecosystems (Halpern et al., 2008; Mora et al., 2013; Côté et al., 2016) that are difficult to understand and predict (Travers-Trolet et al., 2014; Piroddi et al., 2017). Fishing pressure together with the variability of physical forcing (*e.g.* winds, currents) may affect the structure and functioning of the entire food web due to the propagation of their direct effects through top-down and bottom-up trophic cascades (Cury et al., 2003; Hunt and McKinnell, 2006). Moreover, drivers' interaction may sometimes lead to synergistic effects, stronger than the isolated impact of each of these drivers (Travers-Trolet et al., 2014: Fu et al., 2018). As many marine systems show signs of degradation (Harpern et al., 2008; Bănaru et al., 2010; Piroddi et al., 2017), understanding how fisheries pressure, environmental conditions, and marine species interact is crucial (Côté et al., 2016), and has become a scientific priority to support key national and international conventions for better preserva-

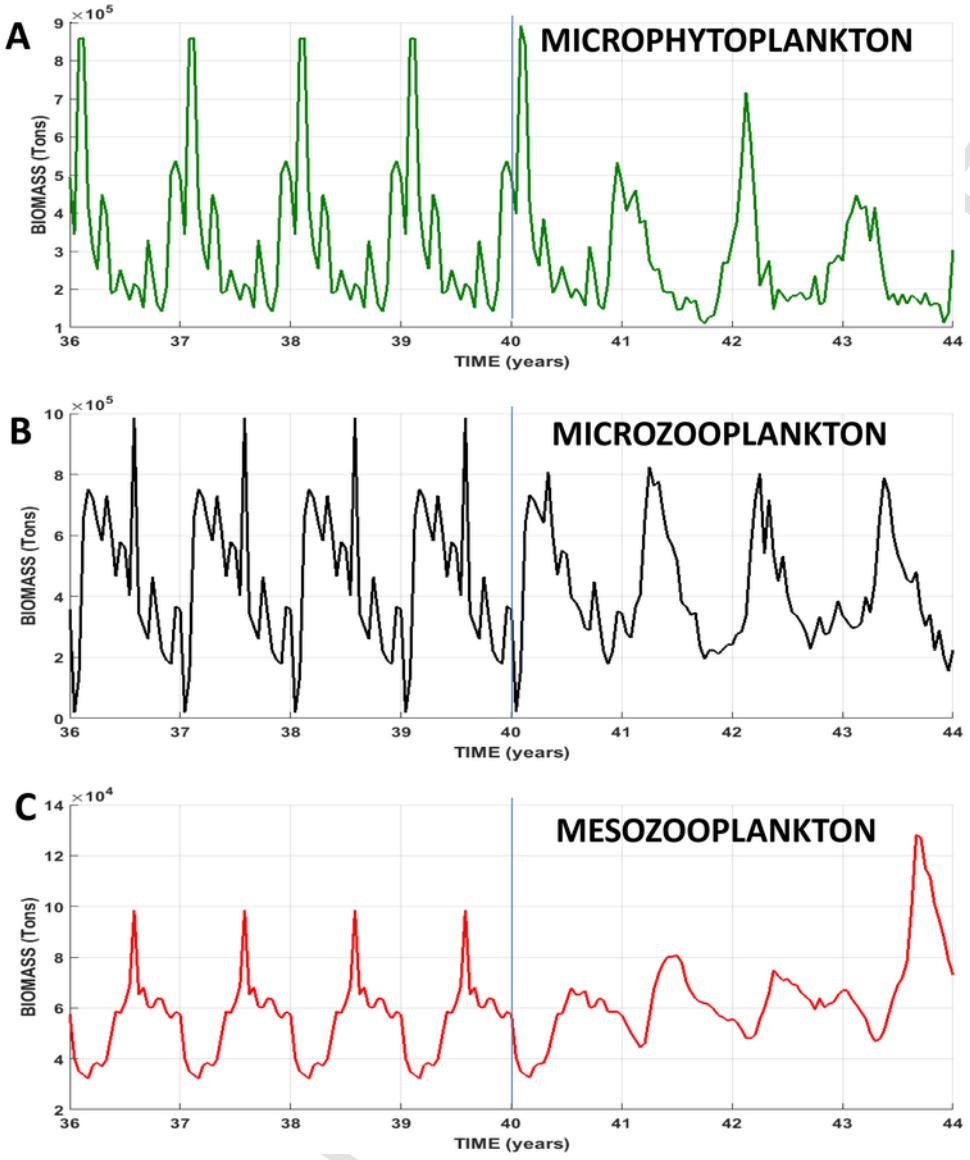

Fig. 1. Temporal dynamics of microplankton and mesozooplankton biomasses during the last eight years of simulation. The solid line represents total biomass summed over the whole modeled domain. The vertical line delimits two periods with different coupling techniques between the Eco3M-S LTL model and the OSMOSE-GoL HTL model: one-way forcing mode from years 36 to 39 and two-ways coupling mode from years 40 to 43.

Table 1
Plankton biomass (in tons) preyed upon by HTL species. For years 36–39 (one-way forcing mode), the mean (± standard deviation) prey biomass annually eaten is reported. For years 40–43 (two-ways coupling mode), the annual plankton biomass preyed upon by HTL species is given. The three main size classes of predators (by decreasing order of ingested prey biomass) are indicated in abbreviations. K: northern krill, $S_{<3}$: European sprat <3 cm, $A_{<3}$: European anchovy <3 cm, $A_{3\text{-}8}$: European anchovy (3–8 cm), $A_{>8}$: European anchovy >8 cm, $P_{<3}$: European pilchard <3 cm, $P_{3\text{-}12.5}$: European pilchard (3–12.5 cm), $P_{>12.5}$: European pilchard >12.5 cm. NANOPHY = nanophytoplankton, MICROPHY = microphytoplankton, NANOZOO = nanozooplankton, MICROZOO = microzooplankton, MESOZOO = mesozooplankton.

Years	[36-39]	40	41	42	43
		(2001)	(2002)	(2003)	(2004)
NANOPHY	**1.47 ± 0.04** $A_{<3}$,$S_{<3}$,K	**2.10** $A_{<3}$,$S_{<3}$,K	**2.13**	**1.87**	**1.98**
MICROPHY	**24636 ± 180** $P_{3\text{-}12.5}$,$P_{>12.5}$,K	**26832** $P_{3\text{-}12.5}$,$P_{>12.5}$,K	**19357** $P_{>12.5}$,$P_{3\text{-}12.5}$,K	**19275** K,$P_{3\text{-}12.5}$,$P_{>12.5}$	**16653** K,$A_{3\text{-}8}$,$P_{3\text{-}12.5}$
NANOZOO	**0.133 ± 0.004** $S_{<3}$,$A_{<3}$,K	**0.139** $S_{<3}$,$A_{<3}$,K	**0.055** $A_{<3}$,$S_{<3}$,K	**0.046** $S_{<3}$,K,$A_{<3}$	**0.032** $A_{<3}$,$S_{<3}$,K
MICROZOO	**29238 ± 1514** $P_{3\text{-}12.5}$,$P_{>12.5}$,$A_{>8}$	**28127** $P_{3\text{-}12.5}$,$P_{>12.5}$,$A_{>8}$	**24444** $P_{>12.5}$,$P_{3\text{-}12.5}$,$A_{>8}$	**22672** $P_{3\text{-}12.5}$,$P_{>12.5}$,$A_{3\text{-}8}$	**20033** $A_{3\text{-}8}$,$P_{3\text{-}12.5}$,$P_{>12.5}$
MESOZOO	**4714 ± 9** $A_{>8}$,K,$P_{3\text{-}12.5}$	**4254** $A_{>8}$,$P_{>12.5}$,$P_{3\text{-}12.5}$	**4836** $P_{<3}$,$A_{>8}$,$P_{>12.5}$	**4682** $P_{<3}$,K,$P_{>12.5}$	**5572**

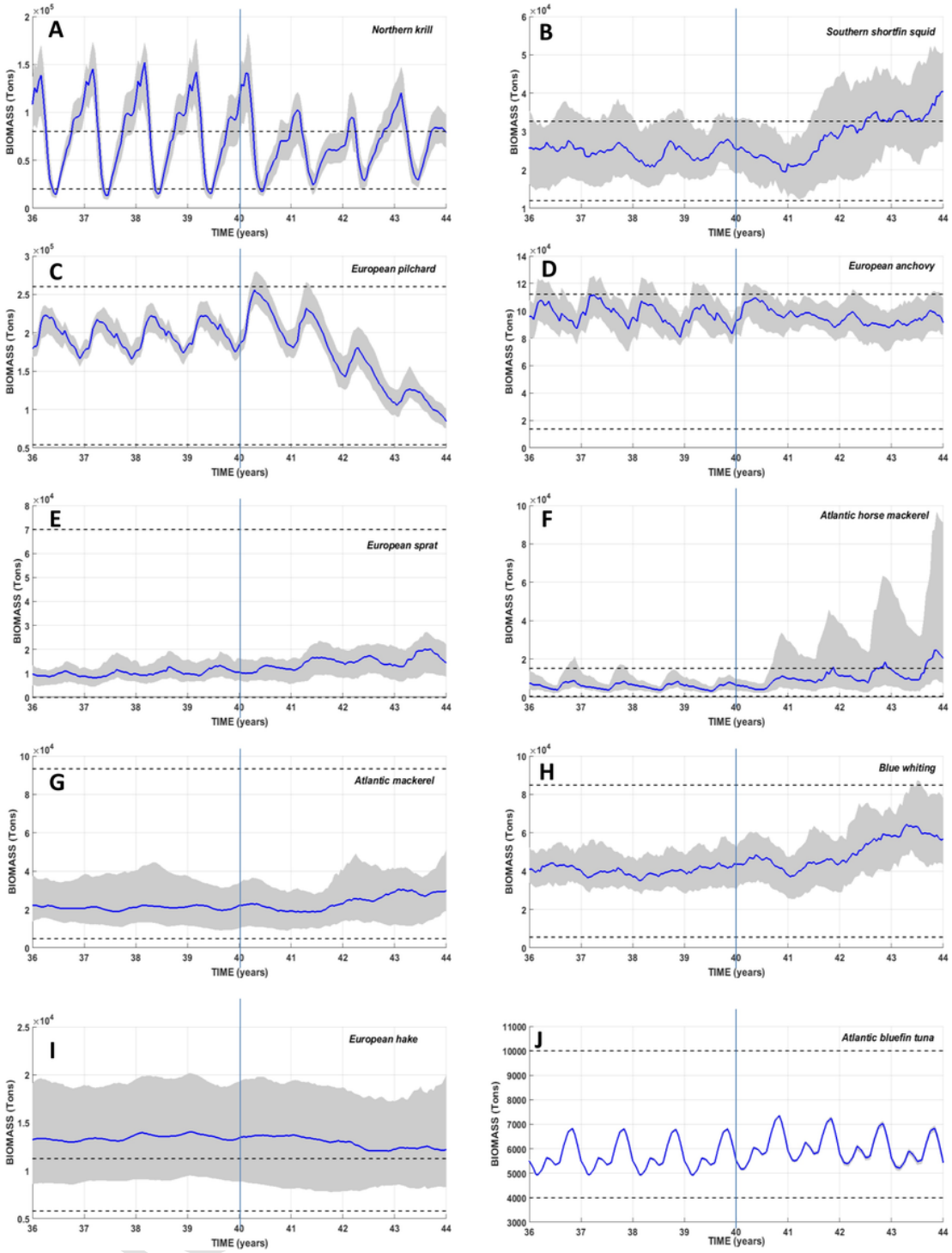

Fig. 2. Temporal evolutions of the simulated total biomass of the 10 HTL species during the last eight years of simulation over the whole modeled domain. The vertical line delimits the temporal period of coupling technique between the Eco3M-S LTL model and the OSMOSE HTL model: coupled run in the one-way forcing mode from years 36 to 39 and in the two-ways coupling mode from years 40 to 43. The solid line shows the median value computed from the 50 simulation replicates. The lower and upper limits of the grey envelope delineate the 0.25 and 0.75 (respectively) percentiles computed from the 50 replicates. The two horizontal dotted black lines represent the range of observed biomass (Bănaru et al., 2019).

tion of natural ecosystems and sustainable use of biodiversity resources (*e.g.* European Marine Strategy Framework Directive; Convention on Biological Diversity, Inter-governmental Platform on Biodiversity and Ecosystem Services).

The semi-enclosed Mediterranean Sea has been considered as a hotspot for marine biodiversity (*e.g.* Bianchi and Morri, 2000; Coll et al., 2010) but it is also a "hotspot" for climate change (*e.g.* Giorgi, 2006; The MerMex Group et al., 2011). In parallel, the Mediterranean Sea, owing to its location between Africa, Europe and Asia, is under siege from many anthropogenic alterations such as the overexploitation of resources, habitat loss and various forms of pollution due to the rapid expansion of the demography all along its coasts (*e.g.* Coll et al., 2010, 2012; Lötze et al., 2011).

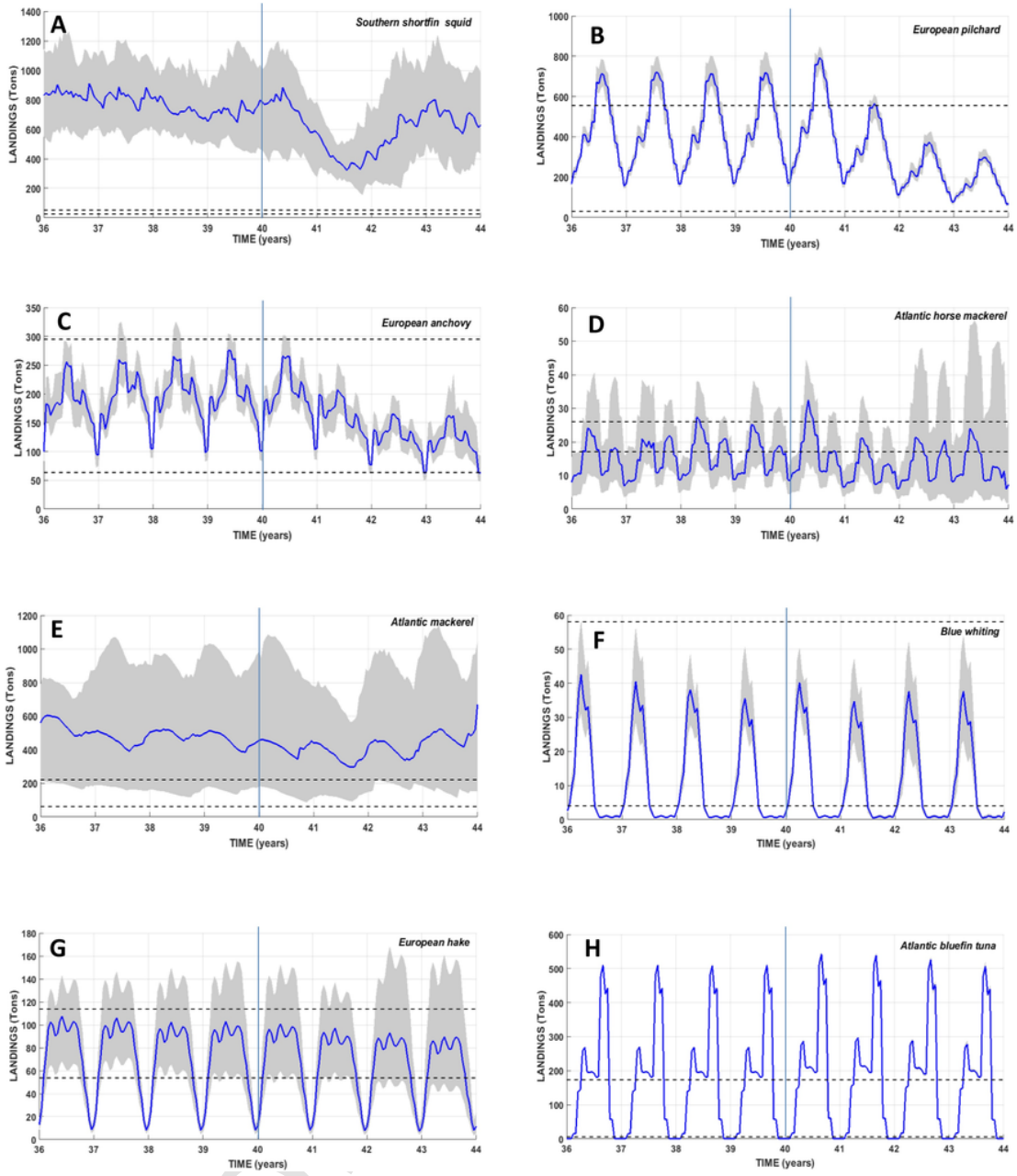

Fig. 3. Temporal evolutions of the simulated total landings of the 10 HTL species during the last eight years of simulation over the whole modeled domain. The vertical line delimits the temporal period of the coupling technique between the Eco3M-S LTL model and the OSMOSE-GoL HTL model: coupled run in the one-way forcing mode from years 36 to 39 and in the two-ways coupling mode from years 40 to 43. The solid line shows the median value computed from the 50 simulation replicates. The lower and upper limits of the grey envelope delineate the 0.25 and 0.75 percentiles computed from the 50 simulation replicates. The two horizontal dotted black lines represent the range of observed landings (Bănaru et al., 2019).

In the Northwestern Mediterranean Sea, the Gulf of Lions (GoL) is characterized by a wide and shallow shelf. This area is one of the most productive zones of the Mediterranean Sea (*e.g.* Bosc et al., 2004) owing to heavy year-round nutrient inputs, mainly from the Rhone River (Lefèvre et al., 1997). It is thus an important feeding area for many resident and migratory High Trophic Level (HTL) species. As a result, 20% of the French fishing fleet operates in the GoL and 90% of the French Mediterranean landings take place in this area (Demaneche et al., 2009). Many fish species of commercial interest have been intensively exploited on the GoL continental shelf over the past decades by French and Spanish fleets using multi-specific artisanal gears (Farrugio et al., 1993; Sacchi, 2008). In this area, a study based on the ECOPATH mass-balance model suggested that some fish species may be overfished with respect to the amount of biomass necessary for the functioning of the food web (Bănaru et al., 2013). Forage species, such as European pilchard and European anchovy, representing usually more than 50% of the total catches in this area, are one of the most important prey groups, being a major trophic link between plankton and top predators as some fish species, seabirds and mammals (Bănaru et al., 2013). However, over the last ten years, and despite the decrease in fishing pressure, the mean size and body condition of European pilchard and European anchovy have declined (Van Beveren et al., 2014; Saraux et al., 2018). Recent studies on their diet (Le Bourg et al., 2015) showed that they probably consume smaller prey than in the past, and that they maybe in competition with the European sprat, a non-commercial planktivorous fish which has strongly increased in biomass during recent years in this area. Some interesting questions arise from these ob-

Table 2
Values of the maximum HTL-induced mortality rates ($\frac{a_p}{\Delta t}$), LTL mortality rates (m_p) and ratio of two parameters on plankton four groups. NANOPHY = nanophytoplankton, MICROPHY = microphytoplankton, NANOZOO = nanozooplankton, MICROZOO = microzooplankton, MESOZOO = mesozooplankton (see Banaru et al., 2019 for the definitions of a_p and Δt).

	$\frac{a_p}{\Delta t}$	m_p	Ratio
	(d^{-1})	(d^{-1})	
NANOPHY	0.0394	0.000	–
MICROPHY	0.0148	0.075	0.197
NANOZOO	0.0207	0.043	0.481
MICROZOO	0.0105	0.070	0.150
MESOZOO	0.0099	0.033	0.300

servations, such as why there has been a higher rate of consumption of smaller prey by planktivorous fishes over the past few years in this area? Have these small planktonic prey species been more abundant in recent years? And if so, is environmental forcing (winds, hydrodynamics) and its variability at different frequencies responsible for this alteration of the plankton community? In this context, the trophic and especially size-based trophic interactions within the food web and the impact of the environmental conditions on these interactions are of crucial importance in order to understand the functioning and recent evolution of the GoL ecosystem.

Models that integrate the representation of the whole ecosystem from the dynamics of the physical environment to that of the highest trophic levels, the so-called end-to-end (E2E) models (see Rose, 2012 for an accurate definition), are useful tools to address the aforementioned ecological questions.

In the present study, the E2E model chosen to explore these questions is the individual- and size-based model OSMOSE (Shin and Cury, 2004) with a configuration dedicated to the GoL, named OSMOSE-GoL, that has been recently parameterized, calibrated and confronted to observations (see details in the companion paper Bănaru et al., 2019). One of the strengths of this configuration is to account for a fully dynamic two-ways coupling between the models of Low Trophic Level (LTL) organisms (usually biogeochemical models) and HTL organisms. In this configuration of coupling, outputs of plankton groups provided by the LTL model serve as prey fields for the HTL organisms, which return an additional predation mortality in the plankton groups. The im-

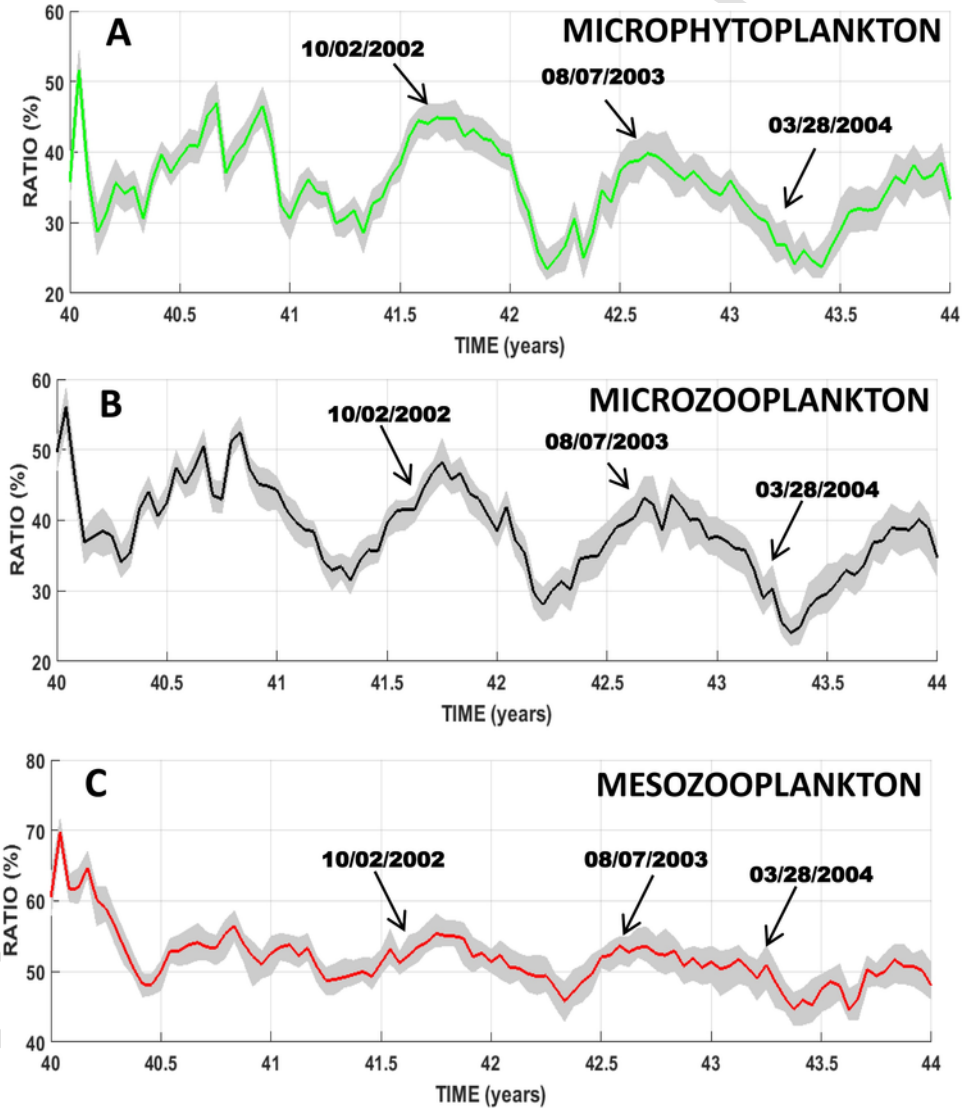

Fig. 4. Temporal evolutions of the HTL predation pressure (see Section 3.4. for a detailed definition) on mesozoo- and microplankton groups over the whole modeled domain under the two-ways coupling mode. The solid line shows the median levels computed from the 50 simulation replicates. The lower and upper limits of the grey envelope delineate the 0.25 and 0.75 percentiles computed from the 50 simulation replicates. Black arrows and associated dates indicate the dates of spatial distributions showed on Figs. 5–8.

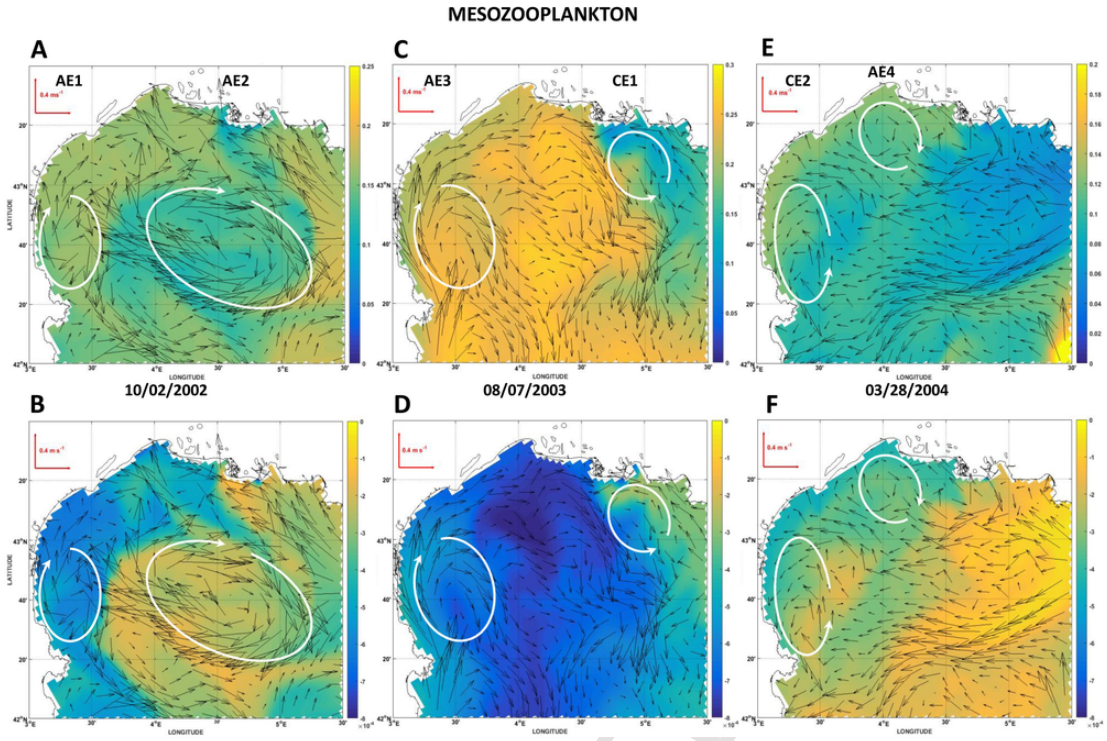

Fig. 5. Surface fields of mesozooplankton modeled biomass (mmol m^{-3}) at three selected dates along the simulation. For a given date, upper panels show plankton biomass resulting from the OSMOSE-GoL model (two-ways coupling mode between HTL and LTL models). The lower panels show patterns of differences (OSMOSE-GoL minus LTL model) in biomass (mmol m^{-3}). Vectors represent the surface field of currents at the corresponding date. The locations of hydrodynamic structures of interest as mesoscale cyclonic (CE) and anticyclonic (AE) eddies are indicated by the white ellipses.

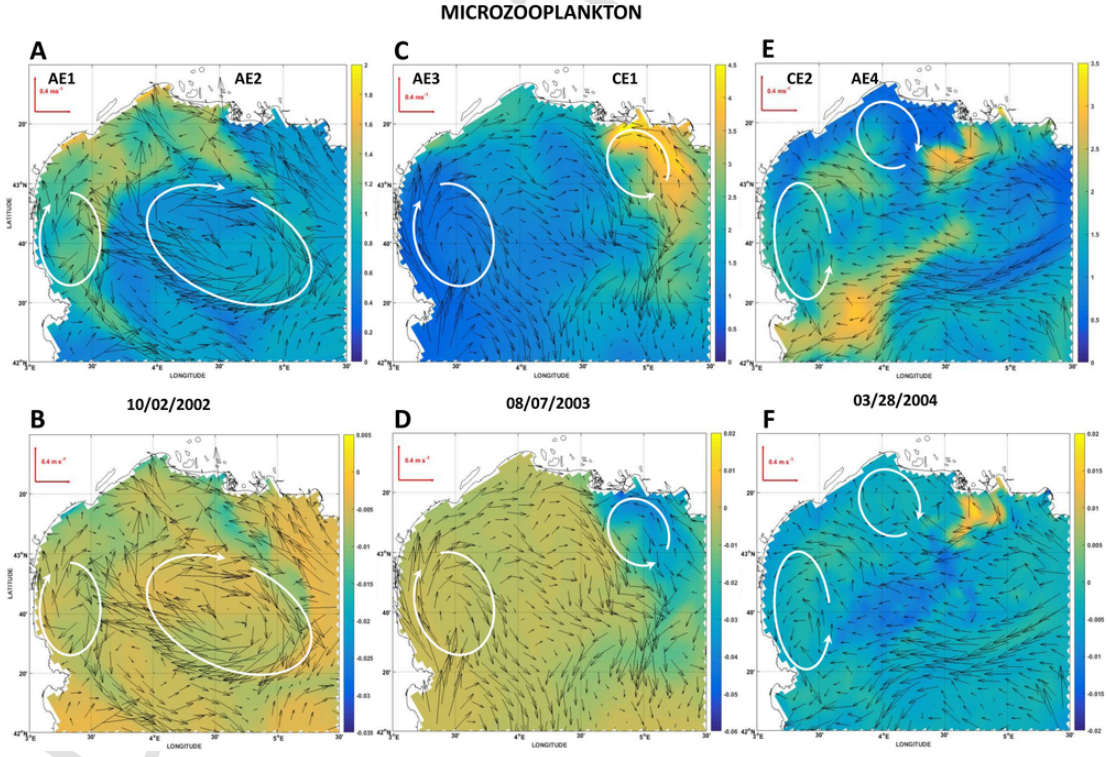

Fig. 6. Same caption as Fig. 5 for microzooplankton biomass (in mmol m^{-3}).

plementation of E2E models has rarely been undertaken in a dynamic two-ways coupling between LTL and HTL models but rather in a one-way forcing mode with outputs from biogeochemical models being used as forage fields for HTL organisms without any feedback on the LTL biomass and distributions. As a result, the effects of the type of models' coupling (with or without feedbacks from HTL to LTL organisms) on ecosystem dynamics have only been documented for the ma-

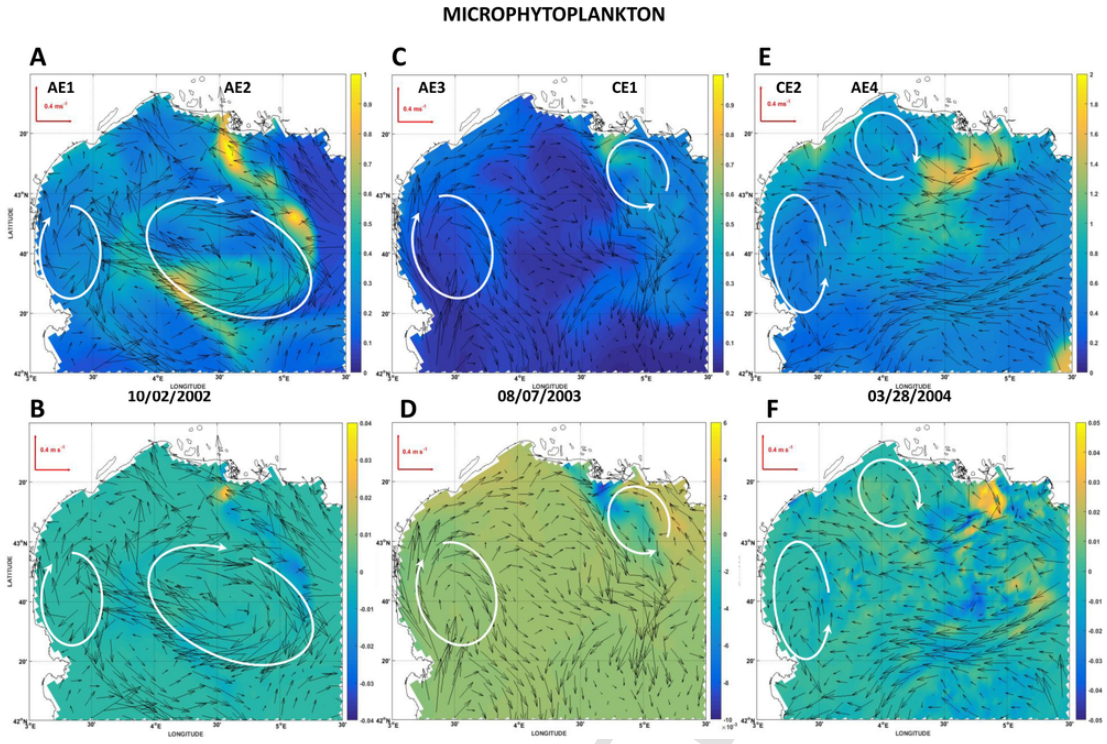

Fig. 7. Same caption as Fig. 5 for microphytoplankton biomass (in mmol m^{-3}).

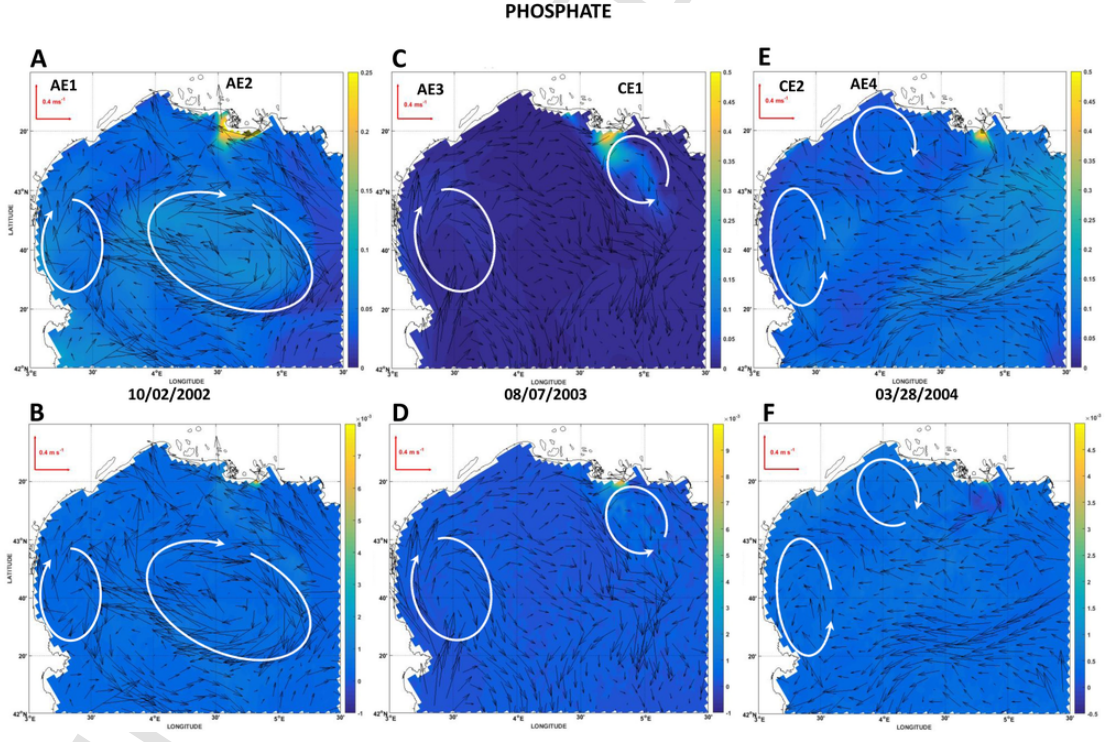

Fig. 8. Same caption as Fig. 5 for phosphate concentrations (in mmol m^{-3}).

rine ecosystem of the Benguela Current (Travers-Trolet et al., 2009, 2014) to the best of our knowledge.

The aims of the present study are therefore the following. (i) To assess the impact of the two-ways coupling between the LTL and HTL sub-models on the outputs of the E2E model. This evaluation will be undertaken through the analysis of changes in the temporal dynamics of the biomass and landings of living resources, in predation pressure on plankton groups and in the resulting trophic cascade effects. (ii) To evaluate the order of magnitude and potential impacts of the two-ways coupling and hydrodynamic processes (meso-scale eddies, region of freshwater influence by Rhone River) on the spatial distribution of plankton and nutrients. (iii) To propose hypotheses to enlighten the environmental causes of the observed fluctuating stocks of certain fish species (*e.g.* European anchovy, European pilchard, and European

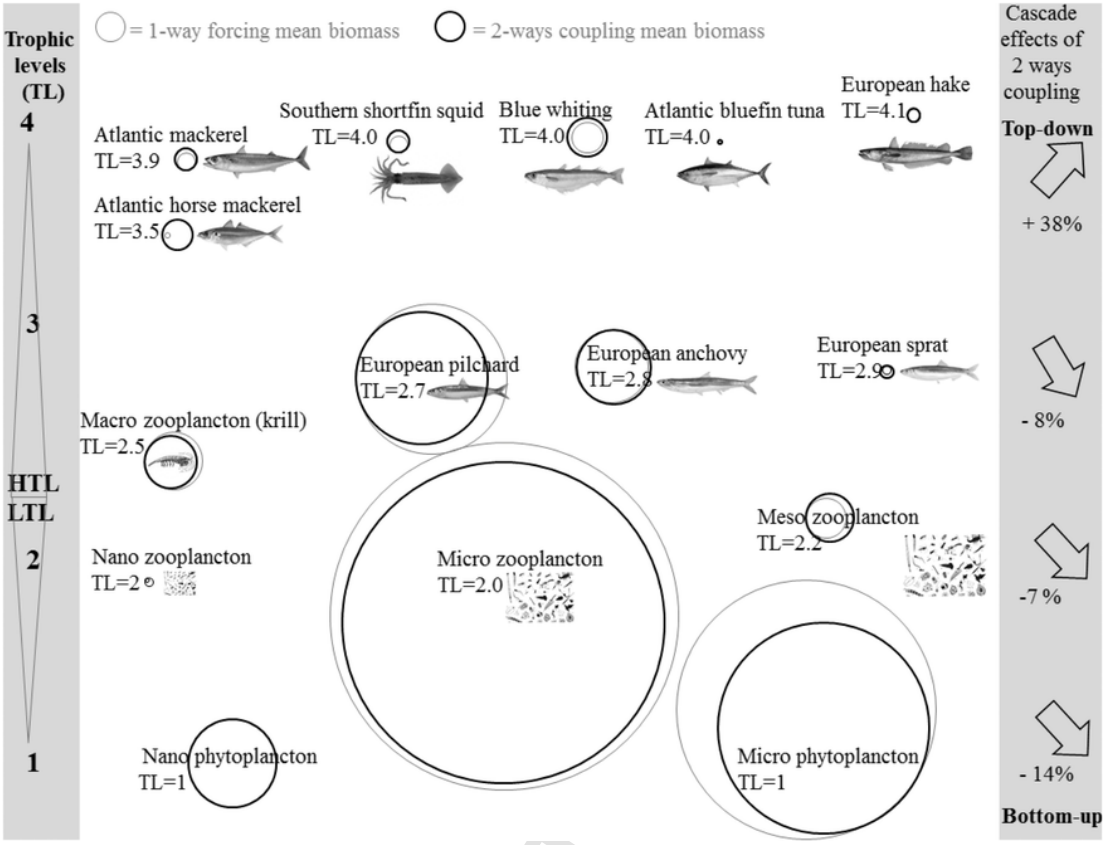

Fig. 9. Cascade effects on food web groups and species biomass and food web controls between the two-ways coupling mode *vs.* one-way forcing mode. Arrows indicate change in biomass by trophic level. Circle size is proportional to their mean biomass. Grey circles indicate the mean biomass in the one-way forcing mode (years 36–39) and black circles indicate the mean biomass in the two-ways coupling mode (years 40–43).

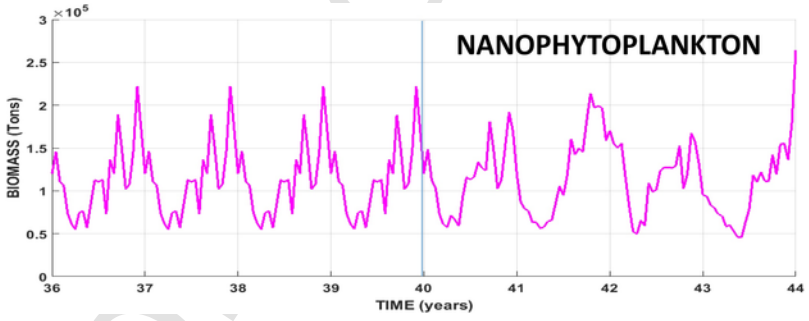

Fig. A1. Temporal dynamics of nanophytoplankton biomasses during the last eight years of simulation. The solid line represents total biomass summed over the whole modeled domain. The vertical line delimits two periods with different coupling techniques between the Eco3M-S LTL model and the OSMOSE-GoL HTL model: one-way forcing mode from years 36 to 39 and two-ways coupling mode from years 40 to 43.

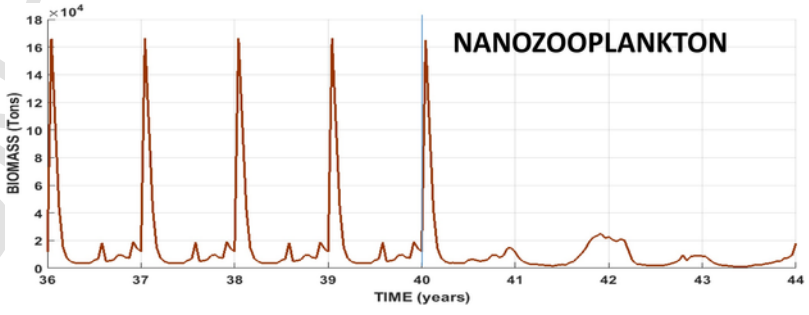

Fig. A2. Same caption as Figure A.1. for nanozooplankton biomasses.

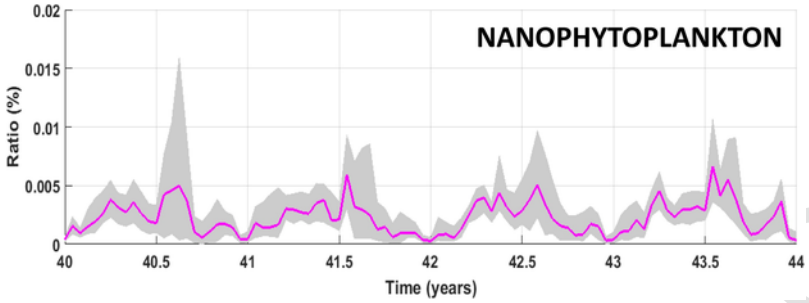

Fig. A3. Temporal evolutions of the HTL predation pressure (see Section 3.4. for a detailed definition) on nanophytoplankton groups over the whole modeled domain under the two-ways coupling mode. The solid line shows the median levels computed from the 50 simulation replicates. The lower and upper limits of the grey envelope delineate the 0.25 and 0.75 percentiles computed from the 50 simulation replicates.

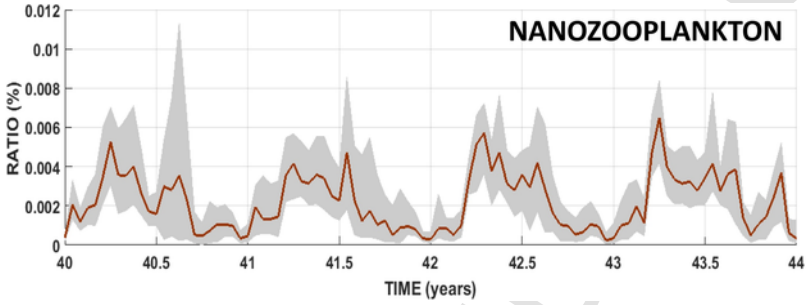

Fig. A4. Same caption as Fig. A3 for nanozooplankton.

sprat). The E2E model was run over a four-year period characterized by contrasted environmental conditions, involving a high interannual variability of the biomass of certain plankton groups. The analysis of this run may enable to disentangle the respective roles of bottom-up and top-down processes on the seasonal and interannual dynamics of HTL organisms. This type of analysis is crucial to raise our capacity in moving towards Ecosystem Based Management of the fisheries in the GoL marine area.

2. Methods

The OSMOSE-GoL model that has been previously described, parametrised, calibrated and evaluated in the companion paper (Bănaru et al., 2019), is used in this study to achieve the aforementioned aims. This E2E model is composed of two sub-models. The first is the Eco3M-S/Symphonie model (Campbell et al., 2013) that represents the dynamics of LTL organisms influenced by hydrodynamics and meteorological processes. The second is the individual-based model OSMOSE (Shin and Cury, 2004; Grüss et al., 2015) that simulates the dynamics of HTL organisms. The design of the numerical experiment is detailed in the companion paper (Bănaru et al., 2019), but its main points are reminded in the following for sake of clarity. The OSMOSE-GoL is firstly calibrated using an optimization technique relying on an evolutionary algorithm and a likelihood-based objective function (Oliveros-Ramos and Shin, 2016). The calibrated model is then run in the one-way forcing configuration and feed in loop on the numerical fields of LTL biomass for year 2001, until a realistic equilibrium is reached in the levels of HTL outputs (Bănaru et al., 2019). This equilibrium is reached after a period of 35 years that is considered as a spin-up period. Following this spin-up period, the OSMOSE-GoL model is run first in the one-way mode during years 36 to 39 and then in the two-ways coupling mode by receiving the numerical fields of LTL biomass from years 2001 to 2004 (corresponding to years referred to as 40 to 43 hereafter). A set of 50 simulations was launched to account for the stochasticity of the OSMOSE model. The one-way forcing period (years 36 to 39) as well as the period of two-ways coupling mode (years 40 to 43) have been considered for analysis in the following sections. Mean, median (and associated percentiles) values are used to synthetically present and analyze the outputs of the model.

3. Results

3.1. Temporal dynamics of plankton biomass

The annual cycles of microphytoplankton (Fig. 1A) show the highest levels of biomass along winter period and at the onset of spring in the one-way forcing mode. The summer season is characterized by the lowest biomasses and weakest variations. Autumn is characterized by an increase in biomass that is of lower intensity than that of the spring. A more pronounced interannual variability of seasonal dynamics can be noted under the two-ways coupling mode. The intensity and duration of winter peak are very variable depending on the year. The sharp decrease in biomass occurring later during spring is always present. Autumnal peak can be present on some years (*e.g.* 40, 42) while absent on the other ones. The microphytoplankton biomass yearly eaten (Table 1) is on average ~24.6 10^3 tons (s.d. 180 tons) in the one-way forcing mode which represents from 3 to 16% of the available stock. Over year 40, the biomass eaten increases to nearly 27 10^3 tons, that is 18% of the available stock. The microphytoplankton biomass annually consumed by predators significantly falls down to 19 10^3 tons during the following two years 41 and 42, and drastically decline again to 16.7 10^3 tons during year 43. Whatever the coupling mode, the main predators of microphytoplankton are the two largest classes (>3 cm) of European pilchard and northern krill. However, in year 43, the intermediate size class of European anchovy (3–8 cm) appears to be the second most important predator, at the expense of the largest European pilchard (>12.5 cm).

The annual cycle of microzooplankton biomass (Fig. 1B) in the one-way forcing mode shows sharp variations of biomass throughout the years while, in the two-ways coupling mode, the variability is less marked. In the one-way forcing mode, biomass is at its minimum at the beginning of winter then sharply rises up to 7.5 10^5 tons. The rest of

the year is characterized by a decreasing trend of biomass until the end of autumn, punctuated by large and rapid variations such as a recurrent summer peak of biomass. The last three years of simulation in the two-ways coupling mode have the common point of showing a minimum biomass moved forward during autumn and a delayed peak occurring at the end of winter (years 41 and 42) or even during spring (year 43). The amount of microzooplankton yearly eaten is slightly higher than 29 10^3 tons on average in the one-way forcing mode (Table 1) and decreases gradually throughout the simulated years in the two-ways coupling mode down to *ca.* 20 10^3 tons (year 43), then representing *ca.* 10% of the autumnal minimum. The largest size classes of European pilchard (>3 cm) and European anchovy (>8 cm) are, on average, the main predators of microzooplankton in the two coupling modes. However, it can be noted that there is a certain decrease in the predator size (*e.g.* European anchovy) since the intermediate size class appears to be one of the three main predators, at the expense of the largest size class from year 42.

As for microzooplankton, the annual cycle of the mesozooplankton biomass (Fig. 1C) in the one-way configuration strongly differs from those occurring in the two-ways mode. In the one-way configuration, minima levels of biomass are found during winter, followed by a sharp increase from spring to summer peaking at the end of summer. Then biomass quickly falls by *ca.* 40% before a slower decrease during autumn, then a sharper fall at the onset of the following winter. The seasonal cycles in the two-ways configuration are marked by a strong interannual variability. While the minimum biomass in winter increases over the years, the seasonal peaks of biomass are reached in spring, summer, autumn of years 42, 41, 43, respectively. The amount of mesozooplankton eaten yearly is 4714 tons on average in the one-way configuration (Table 1), ranging between 5 and 15% of the available stock. In contrast to the dynamics of predation on all other planktonic prey, there is no clear trend in the quantity of mesozooplankton eaten over the years in the two-ways configuration. It is worth noting that the amount of eaten biomass is the highest one (5572 tons) during year 43, in line with the sharp increase in available biomass during the second part of that year (Fig. 1C). The European anchovy (exclusively >8 cm) and European pilchard (all size classes) are the main predators of mesozooplankton. The northern krill can occasionally be the second most important predator, as in years 42 and 43, and in the one-way configuration. It is interesting to note that, while the amount of eaten biomass increases by *ca.* 20% from year 42 to 43, the ranking of the main predators does not change.

The seasonal cycle of the nanophytoplankton biomass (Fig. A1) shows a minimum at the end of winter followed by an increase from spring to the end of autumn. The year-to-year variability of the biomass cycle is marked over the period of the two-ways coupling mode. The amount of nanophytoplankton consumed compared to the available stock (Fig. A1) remains extremely low (<0.004%) whatever the coupling mode considered (Table 1). However, this amount increases by ~40% in the two-ways coupling mode. The smallest size classes of European anchovy, European pilchard as well as northern krill are the main predators of nanophytoplankton whatever the linking mode considered.

The annual cycles of nanozooplankton in the one-way forcing mode (Fig. A2) show an abrupt increase at the onset of winter followed by a sharp drop to very low levels along the rest of the year. Years 41–43 are characterized by a strong erosion of the winter peaks. The nanozooplankton biomass yearly eaten (Table 1) is very low (*ca.* 0.13 tons on average) in the one-way forcing mode and even lower when two-ways coupling is implemented, representing a tiny proportion of the planktonic food (<0.005%). As expected, the smallest sizes (<3 cm) of European sprat and European anchovy as well as northern krill are the main predators of nanozooplankton.

3.2. Temporal dynamics of HTL species biomass

The seasonal dynamics of HTL species resulting from the one-way forcing mode have been already depicted in detail by Bănaru et al. (2019) and only the seasonal cycles produced under the two-ways coupling mode are hereafter described (years 40 to 43 in Fig. 2).

Most of the modeled biomass of HTL species shows interannual changes in median values within the ranges of biomass estimates from field observations, except that of European hake which is slightly overestimated.

The median biomass of northern krill (Fig. 2A) shows wide variations, with the highest and lowest values occurring in winter and the end of spring, respectively. Interannual variability of the seasonal cycle can be noted. For example, the autumnal plateau does not exist during year 42 and show a continuous increase up to a peak of biomass reached during the next winter. This year 43 winter maximum is ~30% higher than those of previous years.

At the onset of the two-ways coupling, the biomass of southern shortfin squid (Fig. 2B) decreases from ~2.5 10^4 tons down to ~2 10^4 tons. The following two years show, on the contrary, a continuous and strong increase in biomass with only slight seasonal variations.

The temporal dynamics of European pilchard (Fig. 2C) show regular seasonal variations, with maxima reached at the onset of spring and minima at the entrance of winter. The yearly range of extreme values is wide, with variations of 30–40% of the biomass. During year 40, the spring maximum of biomass reaches ~2.6 10^5 tons, while the minimum is around 1.80 10^5 tons. The following years then show a global decrease in the biomass levels, with lower and lower spring maxima (<1.25 10^5 tons in year 43).

During year 40, the median biomass of European anchovy (Fig. 2D) shows a seasonal cycle characterized by highest biomass from mid-winter to the end of spring, and lowest biomass during autumn. This seasonal dynamic almost entirely disappears the following years, with spring peaks barely detectable (*e.g.* years 41 and 43).

The seasonal variations in the biomass of European sprat (Fig. 2E) are weak. However, the range of variations is more marked under the two-ways configuration. Highest biomass occurs at the end of spring while the lowest is found at the beginning of winter. The highest median biomass reaches ~2 10^4 tons during year-43, and is almost twice the maximum of year 40.

The dynamic of Atlantic horse mackerel (Fig. 2F) has common points with that of European sprat. Seasonal variations in biomass are weak, but they perceptibly increase under the two-ways configuration. Furthermore, the biomass peaks regularly increase reaching up to *ca.* 2.5 10^4 tons at the autumn end of year 43, that is 35% more than the maximum reached during year 40. In parallel, there is a larger spread of the percentiles range especially towards the high values of biomass.

A very weak seasonal signal can be observed in the simulated biomass of Atlantic mackerel (Fig. 2G). The amplitude of variations between maxima from end of winter to mid-spring and minima from mid-summer to mid-autumn does not exceed ~12%. However, year 41 is characterized by the absence of biomass peak at the end of winter. The last two years show a significant increase in biomass levels by >20% compared to previous years.

The biomass of blue whiting (Fig. 2H) does not show any clear seasonal pattern. Median biomass fluctuates around 4 10^4 tons during year 40 and the three last years are characterized by an increase in the biomass up to 6.5 10^4 tons.

The biomass of European hake (Fig. 2I) does not show any significant seasonal signals. The level of biomass remains almost constant (~1.4 10^4 tons) during years 40 and 41, but a slight decrease (~10%) occurs over the last two years.

The median biomass of Atlantic bluefin tuna (Fig. 2J) shows a marked seasonal cycle. A minimum biomass during winter (˜5000-5500 tons) is followed by a rapid increase up to a first peak at the onset of spring (˜5600-6200 tons). Another minimum biomass occurs at the entrance of summer, and then the annual peak (˜7000 tons) occurs during every autumn. A slight increase in biomass (+10%) is noted, especially during the first three years under two-ways configuration.

3.3. Temporal dynamics of HTL species landings

The temporal dynamics of HTL species landings results from the input parameters of the model and particularly fishing mortality and seasonality that remain constant over the whole modeled period (Bănaru et al., 2019) and of the dynamics of the exploited stocks and the food web interactions.

As in the one-way configuration (Bănaru et al., 2019), the modeled landings of most of the HTL species (except southern shortfin squid and Atlantic mackerel) stand within the ranges of observed data (Fig. 3). Catches of northern krill and European sprat (results not shown) are not computed by the model as they are not landed by fishermen.

The temporal dynamics of HTL species with planktivorous-dominant diet, such as southern shortfin squid (Fig. 3A), European pilchard (Fig. 3B) and European anchovy (Fig. 3C) have in common to show significant changes between year 40 and the following three years. For the latter two species, the seasonality of the landings remains similar, but a significant decline occurs over years 41–43. For the southern shortfin squid (Fig. 3A), both the seasonal cycle and the level of landings change radically. The landings are almost stable during the first part of year 40, and then sharply fall of more than 50% until the middle of year 41. The years 42 and 43 show an increase up to *ca.* 700 tons without a clear seasonal cycle.

The temporal dynamics of Atlantic horse mackerel (Fig. 3D) shows a seasonal cycle composed of two maxima (spring and autumn) and two minima (winter and summer). The spring maximum is considerably higher than that of autumn except in year 42. Year 40 shows the highest spring peak, with landings exceeding 30 tons. In parallel, the winter minimum (˜8 tons) is generally lower than that of summer, except for year 42. The last two years are characterized by a larger spread of the percentiles range especially with regard to the high values of landings during spring.

Landings of Atlantic mackerel (Fig. 3E) increase during autumn and peak at the onset of winter. They then decline slowly down to minimum levels at the end of summer. The seasonal cycle is generally weakly marked. Year 43 shows an overall increase in landings by ˜15%.

The seasonality of landings of blue whiting (Fig. 3F) is almost unchanged in two-ways configuration. Landings are close to zero during autumn, and sharply increase during winter up to their maximum levels. This peak is transient and landings drastically fall in two phases. A small decline first occurs at the onset of summer, followed by a short stabilization, then landings quickly drop to zero during the second part of summer.

Maximum landings of European hake (Fig. 3G) oscillate from mid-winter to the end of summer between 90 and 100 tons during years 40 and 41 and between 80 and 90 tons during years 42 and 43. Autumn is characterized by a sharp decline down to a minimum of ˜10 tons, and the onset of winter shows a sharp increase up to the seasonal maximum.

The pattern of annual dynamics of landings for Atlantic bluefin tuna (Fig. 3H) shows marked seasonal variations and a regular cycle during years 40 to 43. Modeled landings are close to zero from mid-autumn to the beginning of winter which corresponds to the period when bluefin tuna migrates out of this area. A first increase peaking at ˜280 tons follows in spring. A second much higher peak (˜500 tons) then occurs during autumn.

3.4. Temporal dynamics of the HTL predation pressure on the plankton groups

The level of HTL pressure is defined as the ratio between the actual HTL-induced mortality rates and their potential maximum value (Table 2) for each group of planktonic prey.

The median levels of HTL predation pressure on the microphytoplankton group (Fig. 4A) oscillate between 25% and 50%. The second part of the year is generally marked by the highest pressure with a peak during summer. The minimum pressure generally occurs during winter or even spring, as in year 43. There are, however, some significant differences in the annual cycle between years. The seasonal pattern of year 40 shows rather wide and rapid variations, with a minimum occurring at the beginning of winter, followed by an overall increase until reaching two successive peaks of around 47% in summer and autumn. The years 41–43 show (i) lesser variability, and (ii) a decreasing trend of predation characterized, for example, by lower and lower peaks and minima.

The HTL predation pressure on the microzooplankton group (Fig. 4B) oscillates between 25 and 55%. The seasonal pattern mirrors that of microphytoplankton: a predation minimum occurs at the end of winter and is followed by an overall increase from spring to mid-autumn. Year 40 differs from the last three years by wide variations and a marked winter peak. Interannual variability can be also noticed with a pressure minimum moved forward mid-winter (*i.e.* year 42) or delayed mid-spring (*i.e.* years 41, 43). Overall, predation pressure tends to decrease over the simulated four years.

The levels of HTL predation pressure on the mesozooplankton group (Fig. 4C) are *ca.* 50% for most of the simulation period, except at the beginning of year 40 for which ratios exceed 60%. The seasonal pattern generally shows two periods of high pressure. The first one happens in winter and lasts until the onset of spring (*i.e.* year 43), and the second one extends from mid-summer to the end of autumn. The spring period is then rather characterized by a minimum. From years 41 to 43, the winter maximum appears to be strongly reduced while the autumn maximum becomes dominant. As previously noted for the microplankton groups, there is globally a slow decrease in the predation pressure over the simulated period.

The pressure of predation on the nanoplankton groups (Figs. A3 & A4) remains very low (<0.005-0.006%) under the two-ways configuration. The highest pressures of predation generally happen from the onset of the spring to that of autumn (*e.g.* year 43).

3.5. Spatial effects of two-ways coupling on plankton and nutrients

Three snapshots over the simulation period are hereafter shown to illustrate how the two-ways coupling can affect the spatial fields of plankton and even those of nutrients indirectly. Horizontal (Figs. 5–8) fields from February 2002, August 2003 and March 2004 are examined in details because these periods correspond to occurrences of high predation pressure by HTL (Fig. 4) which can involve a direct consumption of plankton prey but also some trophic cascading effects within the LTL. Only the distributions of prey (*i.e.* microphytoplankton, mesozooplankton and microzooplankton) for which the HTL predation pressure was the highest (predation ratio >20%, Fig. 4) over the simulation period are shown as well as those of phosphate contents, a nutrient potentially controlling the level of primary productivity in the GoL (*e.g.* Diaz et al., 2001).

To check the spatial effects of the two-ways coupling on plankton and nutrient, we compared numerical fields from the OSMOSE-GoL model (upper panels of Figs. 5–8) to those without considering any

coupling with OSMOSE model, *i.e.* only resulting from the LTL Eco3M-S/Symphonie model (Campbell et al., 2013). Easier comparisons are made by considering fields of differences (concentrations with HTL predation in two-ways configuration *minus* those without any HTL predation) for plankton and phosphate (lower panels of Figs. 5–8).

The first snapshot to be analyzed happens during the beginning of autumn 2002, and two remarkable hydrodynamic structures under the form of anticyclonic eddies AE1 and AE2 (plots A and B of Figs. 5–8) are present at this period in the GoL. AE1 is of rather small size with an elliptical shape (large semi-axis *ca.* 60 km, small semi-axis *ca.* 40 km), and is entirely located in the southwestern part of the OSMOSE-GoL domain while AE2 is much larger (large semi-axis *ca.* 140 km, small semi-axis *ca.* 70 km) and only partly located in the OSMOSE-GoL domain. These two eddies as well as the **r**egion **o**f **f**reshwater **i**nfluence (ROFI) of the Rhone River (Diaz et al., 2008) mostly shape the distributions of plankton groups and to a lesser degree, that of phosphate. On the whole, the edges of the eddies show difference in biomass or concentrations compared to their center, or even, their surrounding water masses. Depending on the plankton groups considered, these AE (AE2, especially) show at their edges either higher biomass in microphytoplankton, microzooplankton (Figs. 6A & 7A) or lower stocks in mesozooplankton (Fig. 5A) than those around. The ROFI of the Rhone River is clearly identified by the area of phosphate high concentrations (>0.15 mmol m^{-3} on Fig. 8A). The ROFI is characterized by either high microphytoplankton and microzooplankton biomass on its western edge especially, or low mesozooplankton biomass (upper panels and first column of Figs. 5A, 6A, 7A). Several intriguing features appear from the examination of the difference maps (lower panels of Figs. 5–8). When the whole modeled domain is considered, there is generally lower biomass in mesozooplankton and microphytoplankton (Fig. 5B & 7B) and slightly higher microzooplankton and phosphate stocks (Fig. 6B and 8B) in the two-ways coupling mode. The orders of magnitude of differences show strong variations from one plankton group to another and for phosphate: up to a few percent of the available stock for microzooplankton and microphytoplankton, but much lower than 1% for phosphate and mesozooplankton. Spatial gradients on the difference maps are marked for plankton especially in the vicinity of AE2 and the ROFI of the Rhone River. For example, implementing the two-ways coupling had a lower impact on mesozooplankton patterns both in the center and on the edges of AE2 than that modeled on the western part of the GoL shelf (Fig. 5B). By contrast, the impact of considering two-ways coupling on microzooplankton and microphytoplankton patterns was especially high on the edges of AE2 (Fig. 6B & 7B). Within the ROFI of the Rhone River, the account for the two-ways coupling provokes less changes on the two zooplankton groups than those modeled at the edges of AE. The ROFI is also the only zone in this snapshot to show positive differences in microphytoplankton biomass (Fig. 7B) indicating a stronger presence of this prey when the two-ways coupling is explicitly accounted for. Differences in phosphate concentrations are hardly detectable at the edges of AE2. On the whole, the spatial structuration of nutrients and plankton near the small-sized AE1 does not show marked alterations whether the two-ways coupling is activated or not only except for microzooplankton.

The second snapshot to be analyzed happens during the mid-summer 2003 when two remarkable hydrodynamic structures (anticyclonic eddy AE3 and cyclonic eddy CE1, Fig. 5C) are present in the OSMOSE-GoL domain. AE3 is of medium size with an elliptical shape (large semi-axis *ca.* 65 km, small semi-axis *ca.* 50 km) on the southwestern side of the GoL. CE1 is a smaller structure of almost circular shape (radius *ca.* 40 km). CE1 clearly interacts at the time of the snapshot with the ROFI of the Rhone River that can be finely located by the surface distribution of phosphate concentrations (Fig. 8C). The distributions of plankton groups and phosphate on the northeastern and southwestern sides were mainly constrained by CE1 and AE3 respectively. High mesozooplankton biomass (˜0.25 mmol m^{-3}, Fig. 5C) is modeled in the central part of the GoL shelf, while a sharply decreasing biomass gradient occurred in the northeastern part of the shelf owing to the presence of CE1. In the southwestern part of the GoL, mesozooplankton biomass was slightly lower at the edges of AE3 than in surrounding areas.

Surface structuration of microzooplankton biomass is almost the opposite of that of mesozooplankton biomass. High microzooplankton biomass was modeled in the northeastern part of the GoL shelf and near the Rhone River mouth, and the flow of CE1 tended to advect these high biomass southwestwards (Fig. 6C). Similar spatial patterns could be observed for modeled phosphate concentrations (Fig. 8C). Depletion in modeled microphytoplankton was found in the central part of the shelf while the surrounding water masses near eddies showed higher biomass (Fig. 7C). The resulting flow of these two eddies involved an export in microphytoplankton from the coastal area to the offshore zone. In this second snapshot, the two-ways coupling generally provoked the highest losses of plankton in areas of highest biomass whatever the group considered. For example, the northeastern area near CE1 and the Rhone River mouth showed the highest biomass of microphytoplankton and microzooplankton (Figs. 6C & 7C) and also the highest losses in biomass when two-ways coupling is accounted for (Figs. 6D & 7D). In parallel, areas for which losses of biomass are the highest ones (*e.g.* CE1, Rhone River mouth) show a net gain in phosphate at the surface when two-ways coupling is accounted for (Fig. 8D). As noted for the first snapshot analyzed, the orders of magnitude in the differences of biomass strongly vary depending on the prey considered: gains or losses do not exceed 1% of the available stock for microphytoplankton and mesozooplankton while they can reach a few percent of the biomass of microzooplankton.

The third snapshot at the beginning of spring 2004 shows the presence of two remarkable hydrodynamic structures (cyclonic eddy CE2 and anticyclonic eddy AE4, Figs. 5E, 6E, 7E, 8E). AE4 is of small size with a circular shape (radius *ca.* 40 km) in the north central part of the GoL. CE2 is a medium sized structure of elliptical shape (large semi-axis *ca.* 75 km, small semi-axis *ca.* 30 km) that is located in the southwestern part of the GoL shelf. During this snapshot, the ROFI of the Rhone River is shaped by the phosphate surface distribution (Fig. 8E) which appeared to be spatially reduced near the mouth. Over the OSMOSE-GoL domain, mesozooplankton biomass is higher along the coastline (Fig. 5E). The cyclonic and anticyclonic flows of the two eddies tend to spread mesozooplankton on the shelf eastward and southward, respectively. The spatial distribution of microzooplankton biomass is patchy in this snapshot (Fig. 6E). It shows complex spatial patterns characterized by either high biomass as in the central part of the shelf between the two eddies and off the Camargue coast, or low biomass along the shoreline of the GoL. Two main strips of high microphytoplankton biomass are modeled (Fig. 7E). The first one is located along the western coast of the GoL near Cap d'Adge, and the second has a similar location to that of microzooplankton off the Camargue coast with a marked southward spreading. Between these two strips, a large area on the central part of the shelf is rather depleted in microphytoplankton, suggesting that the flows of eddies act as a physical barrier limiting connections between the coastal and offshore areas. Except for the vicinity of the Rhone River mouth, characterized by very high phosphate contents (>0.4 mmol m^{-3}, Fig. 8E), the GoL shelf shows moderate concentrations around 0.2 mmol m^{-3} mainly in its eastern part. From the examination of difference maps, the configuration of two-ways coupling systematically involves lower biomass of mesozooplankton (Fig. 5F) than those without considering any coupling. The effects induced by the two-ways coupling decrease from the western to the eastern edge of CE2 but at the opposite, there are no particular impacts associated with AE4. As for the two previous snapshots, strongest effects of two-ways coupling generally match regions of highest mesozooplankton biomass but overall, the biomass losses re-

main very low, less than 0.5% of the available stock (Fig. 5F). By contrast, most of the zones with high microzooplankton biomass (*e.g.,* central shelf, Camargue coast) are rather characterized by gains in biomass when considering the two-ways coupling (Fig. 6F). The losses in biomass can reach 1–2% of the available stock on the shelf break area while gains do not exceed more than 0.5% off the Camargue coast, for example. In contrast to other plankton groups, the impacts of two-ways coupling on the microphytoplankton distributions are not clearly correlated with the levels of its available biomass. For example, the region of high biomass located off the Camargue coast is both characterized by gains at its eastern edge and losses at its southwestern edge (Fig. 7F). The changes due to the two-ways coupling are relatively important during this snapshot, since the fraction of gain or loss is never lower than 1% and can reach several percent of the available stock. The two-ways coupling do not induce particular changes in phosphate concentrations in relation with the presence of eddies (Fig. 8F). On the whole, there are only minor gains in phosphate near the Rhone River mouth when HTL and LTL models are coupled.

3.6. Effects of considering two-ways coupling on the food web functioning

A similar food web organization is found between the one-way forcing and the two-ways coupling periods (Bănaru et al., 2019), *i.e.* there are no differences concerning the main prey of the HTL species (Fig. 9). Trophic levels do not change between the two configurations for all the species (Bănaru et al., 2019).

Some small differences (less than 5%) can be noticed with lower flows of consumption between microzooplankton and juveniles of European anchovy, and between juveniles of European pilchard and adults of Atlantic horse mackerel (results not shown).

However, some small differences in diet (generally less than 5%, values are not indicated) are noted for the two-ways coupling mode compared to the one-way forcing mode, that are detailed hereafter. European anchovy prey more on microzooplankton and less on nano- and microphytoplankton during winter. Juveniles of European sprat prey more on microzooplankton during winter while adults consume more mesozooplankton and less teleost larvae. Predators generally consume smaller prey. Southern shortfin squid, adults of Atlantic horse mackerel, juveniles of European hake consume more mesozooplankton and less teleosts. In the two-ways coupling mode, only Atlantic bluefin tuna increase their percentage of teleost consumption (juveniles and adults of European sprat and blue whiting, and juveniles of European hake).

Higher differences appear for larvae of European pilchard, adults of European sprat, juveniles of Atlantic horse mackerel, juveniles of Atlantic mackerel, juveniles of blue whiting with an increase in their consumption of mesozooplankton (*ca.* 20%, 15%, 13%, 12% and 19%, respectively) while their consumption of teleost larvae decrease, and that of microzooplankton decrease for larvae of European pilchard, juveniles of Atlantic horse mackerel and juveniles of Atlantic mackerel. For example, juvenile Atlantic mackerel's consumption of juvenile European pilchard decreases by 9%. The size distribution of the prey of adult Atlantic mackerel changes as well, with a decreasing consumption of juvenile and adult European pilchard (by 7.5% and 3%, respectively), but an increasing consumption of the larvae stages (by 5%).

In the two-ways coupling mode, the species composition of the prey is less even in the diet of the majority of predators than those in the one-way forcing mode (northern krill, southern shortfin squid, larvae and juveniles of European pilchard, juveniles and adults of European sprat, juveniles of Atlantic horse mackerel, juveniles of blue whiting). Only juveniles of Atlantic mackerel increase the evenness in their prey composition.

In the two-ways coupling mode, the seasonal variability in the prey composition is reduced compared to that of the one-way forcing mode for northern krill, southern shortfin squid, European pilchard, European anchovy, juveniles of European sprat, and juveniles of Atlantic mackerel. Only Atlantic mackerel and adults of European hake show a higher seasonal variability in the two-ways coupling mode.

For all the OSMOSE HTL groups, the interannual variability in prey composition is higher in the two-ways coupling mode than that in the one-way forcing mode.

Even if small changes in flows and diets are noted between the one-way forcing and the two-ways coupling modes, some changes in biomass by trophic level are found between these two periods (Fig. 9). Phytoplankton biomass decreases by 14% mainly related to microphytoplankton. Zooplankton biomass globally decreases by 7%, which may be related to the decrease in microzooplankton biomass, while mesozooplankton biomass slightly increases. Planktivorous teleosts and northern krill biomass decrease by 8%, mainly related to the decreasing biomass in European pilchard and northern krill, while the biomasses of European anchovy and European sprat slightly increase. Globally, high trophic level predatory teleosts and southern shortfin squid increase their biomass by 38%, all of them showing an increasing biomass trend despite the assumption of a constant fishing mortality during the two periods of coupling modes (Bănaru et al., 2019).

4. Discussion

4.1. Interannual variability of hydrodynamics winter/spring conditions in the North-western Mediterranean Sea over the period 2001–2004

A strong interannual variability of the intensity of deep convection and dense water (DW) formation has been observed for a long time (*e.g.* MEDOC Group, 1970; Gascard, 1978) and it is now known, on the basis of modelling studies (*e.g.* Herrmann et al., 2008; Somot et al., 2018), that the main modes of variability are related to the variability of atmospheric conditions during winter. According to the recent study of Somot et al. (2018) that was based on empirical and model-based indicators (*i.e.* mixed layer depth, yearly maximum extension of the convective zone) of the intensity of DW formation in the study area, the period 2001–2004 was characterized by a succession of winter convective phases which were strongly variable in intensity. The 2001 winter period (defined from January to March) showed a weak convective episode, followed by a slightly weaker convective episode in winter 2002. In contrast, the 2003 winter period was characterized by an episode of strong convection. The 2004 winter period showed a convective phase of moderate intensity, much lower than in 2003 but higher than in 2001 and 2002. For at least three decades, it has been observed that the intensity of spring blooms (especially surface extension, export fluxes) in the NW Mediterranean Sea depended on the intensity of the convection process during the preceding winter on the basis of *in situ* data (*e.g.*, San Feliu and Munoz, 1971; Rigual-Hernandez et al., 2013; Severin et al., 2014), and, satellite remote sensing data (*e.g.*, Volpe et al., 2012; Mayot et al., 2016). Results and analyses with regional 3D coupled models (*e.g.,* Herrmann et al., 2013; Auger et al., 2014; Ulses et al., 2016) corroborate these set of observations. In particular, these latter modelling studies and a recent study related to observation data (Mayot et al., 2017) showed that the size structure of the plankton community during the spring bloom and of the yearly primary productivity was closely related to the intensity of the winter convection events, *i.e.* the higher the intensity of the convective sequence, the more the plankton size spectrum moves towards larger cells. This is a major result that may have some crucial consequences on the structure of the HTL community. The present study aimed to analyze these potential consequences over the 2001-to-2004 time-period that was characterized by a marked interannual variability of deep convection (Somot et al., 2018). The ability of the SYMPHONIE hydrodynamics model to correctly reproduce the shelf DW formation in the GoL (Dufau-Julliand et al., 2004; Ulses et al., 2008) as well as the off-

shore DW formation by deep convection in the Northwestern Mediterranean Sea (Herrmann et al., 2008; Herrmann and Somot, 2008; Auger et al., 2014) has been recurrently shown. The version of the Eco3M-S/Symphonie model implemented here is very close to that of Auger et al. (2014) which produced a similar sequence of interannual variability for the convection process to that modeled by Somot et al. (2018).

4.2. Seasonal and interannual bottom-up and top-down effects between the LTL and HTL communities

Most of the five plankton groups considered in this study show seasonal dynamics that is partly influenced by the winter conditions of the DW formation (Figs. 1, A1, A2). The mesozooplankton and nanoplankton biomass is generally decreasing during winter time but with differential rates. For example, the more convective the winter is, the sharper is the decline in nanophytoplankton biomass, but the lower is the decrease in the biomass of nano- and mesozooplankton. For nanoplankton, the rest of the seasonal dynamics was shaped by the winter evolution of their biomass with the most convective winters (*e.g.* 2003, 2004) generally leading to lower biomass ensuing. Microphyto- and microzooplankton are the groups showing an increase in their biomass during the convective winter period. The pattern of seasonal dynamics of microphytoplankton biomass was more sensitive to the interannual variability of the convection process than that of microzooplankton. Indeed, the spring to autumn biomass of microphytoplankton is higher in the case of moderate (2004) to high (2003) convective winters. The relationship between the winter peak and the intensity of DW formation was less clear, since the year 2001 (2002 respectively) showed higher winter maxima than in 2003 (2004 respectively). This set of model outputs on the seasonal dynamics of plankton *vs*. interannual variability of winter convection intensity is very informative because it shows certain deviations relative to the usual pattern observed in recent datasets (Mayot et al., 2017), and from hydrodynamics-LTL models (Auger et al., 2014). Highly convective winters such as 2003 and, to a lesser extent, 2004 do not systematically have a positive (negative respectively) impact on the microphytoplankton and mesozooplankton biomass (microzooplankton, respectively) as usually assumed. In our E2E modelling study, these deviations may be attributable to the HTL predation on the different plankton groups. Indeed, the groups showing the widest divergences with regard to the usual assumed pattern (*i.e*. microplankton, mesozooplankton) are those under the highest pressure of predation by HTL organisms (Fig. 4). A negative impact of moderate-to-high convective winters on the seasonal cycles of nanoplankton biomass was found (Figs. A1, A2), similarly to the aforementioned previous studies, but occasional deviations could be noted from spring to summer when HTL predation pressure reaches the highest levels, especially for nanophytoplankton. This feature is interesting because, while the direct predation due to HTL on nanophytoplankton remains overall very far from its maximum ($<0.01\%$), this process might be able to shape the seasonal cycle of this size class of phytoplankton during spring and summer. Stable isotope studies showed that nanophytoplankton represents the main organic matter source for the entire food web in the GoL (Bănaru, 2015). This group is dominant in terms of biomass in the NW Mediterranean Sea for most of the year (Marty et al., 2002; Siokou-Frangou et al., 2010; Estrada and Vaqué, 2014; Mayot et al., 2017), and according to our results, it is likely to play an important role for fueling the HTL productivity, even though the HTL predation rate appears to be low. The effects of HTL predation on plankton combined with the variable intensity of the convection process offer some new insights on the controls on plankton biomass at certain crucial periods of the seasonal cycle. For example, the recent study of Auger et al. (2014) based on LTL modeling (*i.e.* without top-down control by HTL) showed that the higher the intensity of convection during winter, the lower the stocks of mesozooplankton are, mainly due to the dispersal of predators and prey with increasing mixing. Our study showed contrasting results when two-ways coupling between LTL and HTL models was performed. The winter stocks of mesozooplankton were the lowest during the winters of 2001 and 2002, that are however the least convective winters of the simulation period. These two sets of results are not fundamentally in opposition. A less convective winter may involve more mesozooplankton and, in turn, higher predation by HTL on this plankton group, reducing its stock *in fine,* while a more convective winter would induce higher stocks by lower predation by HTL, due to dispersal of their prey. This scheme of functioning would consecutively result in winter mesozooplankton stocks that are higher during convective winters and lower during less convective winters. This top-down control on mesozooplankton winter biomass is confirmed by the maintenance of high levels of HTL predation pressure (Fig. 4) during the least convective winters (*e.g.* 2001, 2002) of the simulated period. The maximum (minimum respectively) of HTL predation pressure is delayed to autumn (middle of spring respectively) for microplankton as the winter convection decreases in intensity. This may explain why their biomass is the lowest at the end of autumn in 2001 and 2002. But their winter-spring dynamics are harder to decipher because, in addition to the impact of winter convection and top-down control by HTL, microplankton is also a usual prey for mesozooplankton. Then ecological process of trophic cascading has to be also considered as a further driver of seasonal dynamics. For example, if the positive impact of convection on the microphytoplankton stock is only considered, the 2003 winter peak of microphytoplankton should be the highest one of the simulated period, whereas the highest peak was modeled for winter 2001. Strong top-down controls by both HTL throughout autumn 2002 (Fig. 4) and mesozooplankton at the beginning of winter 2003 (Fig. 1), may explain the difference in the peaks of microphytoplankton biomass between winter of 2001 and 2003. This example illustrates that the seasonal dynamics of plankton biomass, especially from winter-to-spring, may result from an intricate combination of top-down controls and convection intensity (bottom-up) in the study area. In the same way, this combination of drivers may also influence the duration of winter-to-spring peaks for microzooplankton.

It is interesting to analyze whether the interannual variability of the winter convection could have some impacts on the seasonal dynamics of the modeled HTL groups, through the spatio-temporal dynamics of their prey, especially. The answer to this question can be found in the analysis of the "who eats what and when?" (Table 1). Northern krill tended to become a major predator of some plankton groups such as microphytoplankton and mesozooplankton during moderate-to-high convective winters (2003 and 2004). European pilchard was also a main consumer of the largest size classes of plankton but this size-based predation pattern changed in relation with the convection intensity. European pilchards of intermediate and large size were generally the first predators of microplankton in years with low-to-very low convective winters, but consumed much less of these prey in years with more convective winters, when the main predators were the intermediate size classes of northern krill and European anchovy. European anchovies, especially those of large size, are one of the three main predators of micro- and mesozooplankton when winter convection tends to be low-to-very low, whereas they exert very low predation on these plankton groups when winters are more convective. On the whole the size-based predation pattern appeared to change towards smaller individuals eating smaller zooplankton and microphytoplankton when the intensity of convection increases. This pattern is in line with recent observations showing that European pilchard and European anchovy were consuming smaller prey than in previous studies (Le Bourg et al., 2015), and is probably one of the main factors explaining the decrease in their body condition and the current small pelagic fisheries crisis (Brosset et al., 2016; Saraux et al., 2018).

Most of the seasonal dynamics of HTL landings and biomass showed a stronger interannual variability in the two-ways coupling mode, but this variability could not be clearly related to changes in the intensity of winter convection. However, modeled variations in the seasonality of LTL groups influenced by winter convection may disrupt the process of predator-prey match (Cushing, 1996) that may impact the recruitment and biomass of the HTL groups.

While the seasonal dynamics of LTL groups have been shown to be partly shaped by the intensity of winter convection, there were no clear relationships with the interannual variability of HTL groups along the simulated time sequence. It is suggested here that the length of the simulation period was probably too short to detect a bottom-up control of the HTL dynamics by the hydrodynamics of the region. Palomera et al. (2007) have shown a positive correlation between European pilchard and European anchovy biomass and the intensity of winter mixing in the Catalan Sea (NW Mediterranean Sea) from a 15-y time-series. Another field study suggested a year and a half time lag between sardine catches and wind mixing in this area (Lloret et al., 2004). The detectability of the response of small pelagic fishes to bottom-up controls might also depend on the recurrence of winters with similar convective intensities as the small pelagic population dynamics emerge from those of several cohorts and age classes. A succession of at least two or three low or high convective winters might be required to observe a clear response of the small pelagic community. This hypothesis should be tested in future works with the present model, but also putting more focus on the recruitment level each year. A recent study by Brosset et al. (2017) found that global environmental indices (such as NAO, Mediterranean indices) could not explain the observed changes in fish landings and the general decline in the condition of small pelagic fish populations in the Mediterranean Sea. According to this study, the observed changes might be rather due to a combination of more local environmental processes and/or combined with anthropogenic factors such as fishing or pollution.

4.3. Spatial structuration of LTL and HTL communities and associated trophic effects in relation with mesoscale hydrodynamics

The present study enabled investigation of the effects of mesoscale hydrodynamics and HTL predation on the distributions of plankton groups and nutrients in the GoL, and indirectly, understanding of the spatial structuration of some HTL groups of interest, such as small pelagic planktivorous fishes (*i.e.* European pilchard, European anchovy and European sprat). Saraux et al. (2014) highlighted a strong overlap of the latter three species distribution (presence/absence) within the GoL, but they also showed a differential density of biomass at local scale due to either potential interspecific avoidance or different sensitivities to local environmental characteristics. Moreover, Le Bourg et al. (2015) and Brosset et al. (2016) showed overlaps in the diet and stable isotope ratios of these three planktivorous species in the GoL probably related to their spatial distribution and prey availability. In parallel some recent studies, based on either coupled biogeochemical-hydrodynamics modelling (*e.g.* Campbell et al., 2013) or field observations (Marrec et al., 2018), revealed an intricate spatial structuration of the plankton community in connection with the presence of mesoscale to sub-mesoscale eddies. Physical processes down to sub-mesoscale can temporarily favor the access to nutrients and light by local alterations of the density gradient involving changes in the ecological niches of plankton species down to minute spatial scale (Cotti-Rausch et al., 2016). Overall, the model results showed that mesoscale eddies were areas of the strongest gradients in plankton concentrations and of the more significant gains or losses of plankton biomass when the two-ways coupling is considered. In such a configuration of coupling, these gradients could be caused by a combination of processes acting together and whose it is rather difficult to decipher their respective roles. As aforementioned, hydrodynamic processes associated to the eddy could act on spatial distributions either mechanically by increasing dispersal or aggregation of plankton through advection and diffusion or/and by locally modifying environmental conditions favoring furtive bloom or at the opposite accelerating senescence of plankton community. Secondly, aggregation of plankton in the vicinity of eddies could have also attracted planktivorous pelagic fish and krill hence enhancing HTL predation around eddies. This predation would then have been able to furthermore shape spatial gradients by a differential consumption of plankton groups according to the size-structure of HTL organisms attracted. And finally, this differential predation could in turn reshape the plankton community in term of abundances or/and size structure by provoking cascading trophic processes within the community itself. On the one hand, the edges of AE detected in the southwestern and central parts of the GoL showed the most important impacts of two-ways coupling whatever the plankton group considered. This result is in coherence with the uplift of nutrients and the subsequent increase in primary productivity on the edges of anticyclonic eddies (Campbell et al., 2013; review of McGillicuddy, 2016). On the other hand, the two-ways coupling only involved minor changes in the plankton distributions around cyclonic eddies in the GoL. This result could be explained by the shorter lifetimes of cyclonic structures generally observed in this area (Flexas et al., 2002; Hu, 2011). The short life span of these eddies might not enable to reach a significant local increase in plankton biomass to attract HTL in particular. Even though in OSMOSE fish do not track food gradients, but local fish movements follow a random walk (equivalent to the diffusion term in a population advection-diffusion model) and their mean spatial distributions are driven by observed data, their opportunistic feeding behavior may increase predation in cells with higher prey density. However, the structuring role of cyclonic eddies on spatial gradients may also depend on their locations in the GoL. The case of CE1 was particularly intriguing due to its location near the Rhone mouth (Figs. 5C, 6C, 7C, 8C). There is a close interaction between the Rhone plume enriched in microplankton and the northeastern edge of CE1 that shapes, by transport, the distributions of plankton biomass and in turn, probably HTL predation in this area of the GoL. The process of biomass aggregation resulting from the presence of an eddy potentially involved strong pressure of HTL predation on microplankton groups. Data set showed that there could be an attractor effect of plankton spatial distribution with higher biomass in the Rhone river plume for juveniles of different fish species (Morfin et al., 2012; Saraux et al., 2014). Our study shows that mesoscale structures and Rhone river inputs may thus play an important role in fish recruitment in the GoL and may be related to recent changes observed in small pelagic fish stocks. This seems to corroborate the hypothesis of a bottom-up control of their stocks (Le Bourg et al., 2015; Saraux et al., 2018).

When examining the surface distributions of phosphate contents, the differences in concentrations involved by the two-ways coupling are in the order of the nanomolar (up to 10 nM near the Rhone mouth). This order of magnitude is within the range of concentrations measured in the GoL (Diaz et al., 2008). Phosphate exerts a control on primary productivity during part of the year in this area (Diaz et al., 2001) and probably shapes the structure of the picoplankton community (Moutin et al., 2002). In this study, the two-ways coupling may impact phosphate distributions indirectly through the HTL activity of plankton predators or grazers. But their metabolism also releases inorganic nutrients and organic matter in the environment (Libralato and Solidoro, 2009), and may, in turn, influence more directly the spatial distributions of nutrients. The roles of HTL activity on nutrient fields is hence accounted for *a minima* in the present work. This type of processes within the HTL community should be taken into account in E2E modelling developments, as, despite the low numbers of eddies, our results highlighted the intricate interactions between mesoscale hy-

drodynamics and the structuration of nutrients, LTL and HTL communities.

4.4. Effects of two-ways coupling on food web functioning and controls

Even if a small portion of the LTL stocks is consumed by HTL species, our results showed that this may however induce large seasonal and interannual variations for most of the model groups. The changes of biomass by trophic level (Fig. 9) induced by the two-ways coupling could be interpreted in the light of two alternative hypotheses:

i) The hypothesis of a dominant bottom-up effect with a decreasing microphytoplankton biomass due to increased convection and reduced stratification (see Section 4.1). This may induce a decrease in the biomass of microzooplankton and in turn that of some planktivorous species such as northern krill and European pilchard. This would partially release predation on mesozooplankton that increased in biomass while competitors of the European pilchard such as European anchovy and European sprat, had also slightly increased in biomass. Mesozooplankton increase may have favoured the recruitment of higher predator species (4^{th} trophic level), which are also planktivorous at juvenile stages, and globally increased their biomass.

ii) The combined bottom-up and top-down effect hypothesis. The large increase in the high predator species biomass (by 38%) may finally induce a top-down feedback on planktivorous species. This second hypothesis seems more plausible, whether if only bottom-up processes were controlling the food web functioning, we could expect a decrease in the biomass of top predators and not an increase. Adults of Atlantic horse mackerel, Atlantic mackerel, blue whiting and southern shortfin squid may contribute by predation to the decreasing biomass of some planktivorous species. The Atlantic bluefin tuna may also be a potential predator for these forage species. Even if Van Beveren et al. (2017) indicated that recent changes in Mediterranean small pelagic teleosts are probably not due to increased tuna predation, our results, in accordance with (Coll et al., 2018) showed that the hypothesis of top-down control by other predators should not be neglected. Planktivorous species are probably concomitantly impacted by top-down (predation) and bottom-up effects (decreasing plankton prey size and quantity).

Synergic effects of climate and fishing have been shown in the Southern Benguela (Travers-Trolet et al., 2014), but to our knowledge this is the first study using and end-to-end model that analyses the temporal and spatial effects of model coupling on both LTL and HTL groups and on food web controls.

5. Conclusion

The impacts of climate variability and fishing on food web complex interactions can be explored comprehensively with E2E models such as OSMOSE-GoL. In the GoL, wind regimes and hydrodynamics processes have a crucial role in the variability of LTL spatial distributions, seasonal and interannual cycles. According to our model results, this variability at different scales in time and space may impact HTL groups' recruitment, biomass and landings. The hypothesis of a bottom-up control could not explain alone the decline in biomass and size of small pelagic fish found in our model results, and that look strikingly similar to recent concerns about fish and fisheries status in the GoL. Our model results suggest that top-down control by top predators, and feedbacks on plankton dynamics should not be neglected.

The use of a fully dynamic two-ways coupling between the models of LTL and HTL organisms revealed interesting results. On the whole, even though small proportions of plankton global stocks were preyed upon by HTL species, some important consequences for the infra-seasonal and annual cycles of both HTL and plankton groups could be observed in the two-ways coupling mode, involving significant changes in biomass, landings and food web interactions by cascading effects. Spatial effects especially the impacts of HTL predation on the plankton fields were less clear except in areas in which primary productivity was high (*e.g.* ROFI) or in the vicinity of mesoscale hydrodynamics structures (*e.g.* eddies). However, these results remain preliminary as the only considered interaction between the LTL and HTL models is made through predation while the vertical integration (*sensu* Shin et al., 2010) between the two models could be made through other processes such as natural mortality and egestion by HTL producing detritus and ensuing remineralization by heterotrophic plankton, or such as excretion of dissolved inorganic/organic nutrients, in turn, made available for the whole plankton community. Predation on HTL larvae by carnivorous zooplankton (especially by gelatinous organisms, not included in this model) may also have to be taken into account. Horizontal biodiversity integration (*sensu* Shin et al., 2010) could also be improved to represent other major functional groups in the GoL ecosystem such as benthic organisms, or invasive species.

Ecosystem-based fisheries management and biodiversity conservation need to rely on the development of more holistic modelling approaches of the ecosystem to account for complex species multidimensional dynamics (spatial, temporal, multispecies) and their interactions. This goes in pair with improvements in data acquisitions, high-frequency automated observations in the field on a variety of components and processes from the physical environment to the biogeochemistry up to the biomass and life histories of higher trophic level species. This would help increasing the degree of realism and confidence in the parameterization of models, and reduce uncertainty in their projections.

Acknowledgements

This study was funded by the EMIBIOS project (End-to-end Modelling and Indicators for BIOdiversity Scenarios, FRB contract no. APP-SCEN-2010-II) and by the EU FP7 project PERSEUS (Policy-oriented marine Environmental Research for the Southern European Seas, Theme "Oceans of Tomorrow" OCEAN.2011-3 Grant Agreement No. 287600). It benefited and contributed to MERMEX WP2 working group scientific discussions and to the MERMEX IPP "Interactions plancton-planctonophages" project. The authors acknowledge T. Ballerini for her contribution to the coupling code and suggestions that improved the parametrization of the OSMOSE-GoL model, the assistance of the staff of the *cluster de calcul intensif HPC* Platform of the OSU Institut PYTHEAS (Aix-Marseille University, INSU-CNRS) for providing computing facilities, as well as M. Libes and C. Yohia for technical assistance. Thanks are also addressed to Michael Paul for English corrections service.

Appendix A.

References

Auger, P.-A., Ulses, C., Estournel, C., Stemmann, L., Somot, S., Diaz, F., 2014. Interannual control of plankton communities by deep winter mixing and prey/predator interactions in the NW Mediterranean: results from a 30-year 3D modeling study. Prog. Oceanogr. 124, 12–27.

Bănaru, D., 2015. Pelagic and demersal foodweb of the Gulf of Lions elucidated by stable isotope analysis. Marseille, 20-22 Octobre 2015. MERMEX WP2, MISTRALS Workshop

Bănaru, D., Harmelin-Vivien, M., Boudouresque, C.-F., 2010. Man-induced change in community control in the north-western Black Sea: the top-down bottom-up balance. Mar. Environ. Res. 69 (4), 262–275. https://doi.org/10.1016/j.marenvres.2009.11.009.

Bănaru, D., Mellon-Duval, C., Roos, D., Bigot, J.-L., Souplet, A., Jadaud, A., Beaubrun, P., Fromentin, J.-M., 2013. Trophic structure in the Gulf of Lions marine ecosystem (North-Western Mediterranean Sea) and fishing impacts. J. Mar. Syst. 111-112, 45–68. https://doi.org/10.1016/j.jmarsys.2012.09.010.

Bănaru, D., Diaz, F., Verley, P., Ballerini, T., Campbell, R., Navarro, J., Yohia, C., Oliveros-Ramos, R., Mellon-Duval, C., Shin, Y.-J., 2019. Implementation of an end-to-end

model the Gulf of Lions ecosystem (NW Mediterranean Sea). I. Parameterization, calibration and evaluation. Ecol. Model. 401, 1–19. https://doi.org/10.1016/j.ecolmodel.2019.03.005.

Bianchi, C.N., Morri, C., 2000. Marine biodiversity of the Mediterranean Sea: situation, problems and prospects for future research. Mar. Poll. Bull. 40 (5), 367–376. https://doi.org/10.1016/S0025-326X(00)00027-8.

Bosc, E., Bricaud, A., Antoine, D., 2004. Seasonal and interannual variability in algal biomass and primary production in the Mediterranean Sea, as derived from 4 years of SeaWiFS observations. Glob. Biogeochem. Cycl. 18 (1), 1–17. https://doi.org/10.1029/2003GB002034.

Brosset, P., Le Bourg, B., Costalago, D., Bănaru, D., Van Beveren, E., Bourdeix, J.-H., Fromentin, J.-M., Ménard, F., Saraux, C., 2016. Linking small pelagic dietary shifts with ecosystem changes in the Gulf of Lions. Mar. Ecol. Prog. Ser. 554, 157–171. https://doi.org/10.3354/meps11796.

Brosset, P., Fromentin, J.-M., Van Beveren, E., Lloret, J., Marques, V., Basilone, G., Bonanno, A., Carpi, P., Donato, F., Čikeš Keč, V., De Felice, A., Ferreri, R., Gašparević, D., Giráldez, A., Gücü, A., Iglesias, M., Leonori, I., Palomera, I., Somarakis, S., Tičina, V., Torres, P., Ventero, A., Zorica, B., Ménard, F., Saraux, C., 2017. Spatio-temporal patterns and environmental controls of small pelagic fish body condition from contrasted Mediterranean areas. Prog. Oceanogr. 151, 149–162. https://doi.org/10.1016/j.pocean.2016.12.002.

Campbell, R., Diaz, F., Hu, Z., Doglioli, A., Petrenko, A., Dekeyser, I., 2013. Nutrients and plankton spatial distributions induced by a coastal eddy in the Gulf of Lions. Insights from a numerical model. Progr. Oceanogr. 109, 47–69. https://doi.org/10.1016/j.pocean.2012.09.005.

Coll, M., Piroddi, C., Steenbeek, J., Kaschner, K., Ben Rais Lasram, F., Aguzzi, J., et al., 2010. The biodiversity of the Mediterranean Sea: estimates, patterns, and threats. PLoS One 5 (8), e11842https://doi.org/10.1371/journal.pone.0011842.

Coll, M., Albo-Puigserver, M., Navarro, J., Palomera, I., Dambacher, J.M., 2018. Who is to blame? Plausible pressures on small pelagic fish population changes in the northwestern Mediterranean Sea. Mar. Ecol. Prog. Ser. https://doi.org/10.3354/meps12591.

Côté, I.M., Darling, E.S., Brown, C.J., 2016. Interactions among ecosystem stressors and their importance in conservation. Proc. R. Soc. Publ. B 283, 20152592https://doi.org/10.1098/rspb.2015.2592.

Cotti-Rausch, B.E., Lomas, M.W., Lachenmyer, E.M., Goldman, E.A., Bell, D.W., Goldberg, S.R., Richardson, T.L., 2016. Mesoscale and sub-mesoscale variability in phytoplankton community composition in the Sargasso Sea. Deep-Sea Res. I 110, 106–122. https://doi.org/10.1016/j.dsr.2015.11.008.

Cury, P., Shannon, L., Shin, Y.J., 2003. The functioning of marine ecosystems: a fisheries perspective. In: Sinclair, M., Valdimarsson, G. (Eds.), Responsible Fisheries in the Marine Ecosystem. pp. 103–124.

Cushing, D.H., 1996. Towards a science of recruitment in fish populations. In: Kinne, O. (Ed.), D-21385 Oldendorf/Luhe. Ecology Institute, Germany, pp. 1–175.

Demaneche, S., Merrien, C., Berthou, P., Lespagnol, P., 2009. Rapport R3 Méditerranée continentale, échantillonnage des marées au débarquement. Méthode d'élévation et évaluation des captures et de l'effort de pêche des flottilles de la façade Méditerranée continentale sur la période 2007-2008. Programme P6 AESYPECHE "Approche écosystémique de l'halieutique" Projet Système d'Informations Halieutiques SIH, IFREMER, France. 54 pp (In French).

Diaz, F., Raimbault, P., Boudjellal, B., Garcia, N., Moutin, T., 2001. Early spring phosphorus limitation of primary productivity in a NW Mediterranean coastal zone (Gulf of Lions). Mar. Ecol. Prog. Ser. 211, 51–62. https://doi.org/10.3354/meps211051.

Diaz, F., Naudin, J.-J., Courties, C., Rimmelin, P., Oriol, L., 2008. Biogeochemical and ecological functioning of the low-salinity water lenses in the region of the Rhone River freshwater influence, NW Mediterranean Sea. Cont. Shelf Res. 28, 1511–1526. https://doi.org/10.1016/j.csr.2007.08.009.

Dufau-Julliand, C., Marsaleix, P., Petrenko, A., Dekeyser, I., 2004. Three-dimensional modeling of the Gulf of Lion's hydrodynamics (Northwestern Mediterranean) during January 1999 (MOOGLI3 Experiment) and late winter 1999: western Mediterranean intermediate Water's (WIW's) formation and its cascading over the shelf break. J. Geophys. Res. 109, C11002https://doi.org/10.1029/2003JC002019.

Estrada, M., Vaqué, D., 2014. Microbial components. In: In: Goffredo, S., Dubinsky, Z. (Eds.), The Mediterranean Sea: Its History and Present Challenges 6, pp. 87–111. https://doi.org/10.1007/978-94-007-6704-1_6.

Farrugio, H., Oliver, P., Biagi, F., 1993. An overview of the history, knowledge, recent and future research trends in Mediterranean fisheries. In: In: Lleonart, J. (Ed.), Northwestern Mediterranean Fisheries. Scientia Mar. 57, pp. 105–119, (2-3).

Flexas, M.M., Durrieu de Madron, X., Garcia, M.A., Canals, M., Arnau, P., 2002. Flow variability in the Gulf of Lions during the MATER HFF experiment (March-May 1997). J. Mar. Syst. 33-34, 197–214. https://doi.org/10.1016/S0924-7963(02)00059-3.

Fu, C., Travers-Trolet, M., Velez, L., Grüss, A., Bundy, A., Shannon, L.J., Fulton, E.A., Akoglu, E., Houle, J.E., Coll, M., Verley, P., Heymans, J.J., John, E., Shin, Y.-J., 2018. Risky business: the combined effects of fishing and changes in primary productivity on fish communities. Ecol. Model. 368, 265–276. https://doi.org/10.1016/j.ecolmodel.2017.12.003.

Gascard, J.-C., 1978. Mediterranean deep water formation, baroclinic eddies and ocean eddies. Oceanol. Acta 1 (3), 315–330.

Giorgi, F., 2006. Climate change hot-spots. Geophys. Res. Lett. 33, L08707https://doi.org/10.1029/2006GL025734.

Grüss, A., Schirripa, M.J., Chagaris, D., Drexler, M., Simons, J., Verley, P., Shin, Y.-J., Karnauskas, M., Oliveros-Ramos, R., Ainsworth, C.H., 2015. Evaluation of the trophic structure of the West Florida shelf in the 2000s using the ecosystem model OSMOSE. J. Mar. Syst. 144, 30–47. https://doi.org/10.1016/j.jmarsys.2014.11.004.

Halpern, B.S., Walbridge, S., Selkoe, K.A., Kappel, C.V., Micheli, F., Agrosa, C.D., Bruno, J.F., Casey, K.S., Ebert, C., Fox, H.E., Fujita, R., Heinemann, D., Lenihan, H.S., Madin, E.M.P., Perry, M.T., Selig, E.R., Spalding, M., Steneck, R., Watson, R., 2008. A global map of human impact on marine ecosystems. Science 319 (19), 948–952. https://doi.org/10.1126/science.1149345.

Herrmann, M., Somot, S., 2008. Relevance of ERA40 dynamical downscaling for modeling deep convection in the Mediterranean Sea. Geophys. Res. Lett. 35, L04607https://doi.org/10.1029/2007GL032442.

Herrmann, M., Somot, S., Sevault, F., Estournel, C., Déqué, M., 2008. Modeling the deep convection in the Northwestern Mediterranean Sea using an eddy permitting and an eddy-resolving model: case study of winter 1986-87. J. Geophys. Res. 113, C04011https://doi.org/10.1029/2006JC003991.

Herrmann, M., Diaz, F., Estournel, C., Marsaleix, P., Ulses, C., 2013. Impact of atmospheric and oceanic interannual variability on the Northwestern Mediterranean Sea pelagic planktonic ecosystem and associated carbon cycle. J. Geophys. Res. Oceans 118, 5792–5813. https://doi.org/10.1002/jgrc.20405.

Hu, Z., 2011. Structures tourbillonnaires à l'ouest du Golfe du Lion : modélisation numérique et mesures en mer. Ph D thesis. Aix-Marseille Université, 181 pp..

Hunt, G.L., McKinnell, S., 2006. Interplay between top-down, bottom-up, and wasp-waist control in marine ecosystems. Progr. Oceanogr. 68 (2-4), 115–124. https://doi.org/10.1016/j.pocean.2006.02.008.

Le Bourg, B., Bănaru, D., Saraux, C., Nowaczyk, A., Le Luherne, E., Jadaud, A., Bigot, J.L., Richard, P., 2015. Trophic niche overlap of sprat and commercial small pelagic teleosts in the Gulf of Lions (NW Mediterranean Sea). J. Sea Res. 103, 138–146. https://doi.org/10.1016/j.seares.2015.06.011.

Lefèvre, D., Minas, H.J., Minas, M., Robinson, C., Williams, P.J.Le B., Woodward, E.M.S., 1997. Review of gross community production, primary production, net community production and dark community respiration in the Gulf of Lions. Deep. Sea Res. Part Ii Top. Stud. Oceanogr. 44 (3-4), 801–819. https://doi.org/10.1016/S0967-0645(96)00091-4.

Libralato, S., Solidoro, C., 2009. Bridging biogeochemical and food web models for an end-to-end representation of marine ecosystem dynamics: the Venice lagoon case study. Ecol. Model. 220, 2960–2971. https://doi.org/10.1016/j.ecolmodel.2009.08.017.

Lloret, J., Palomera, I., Salat, J., Solé, I., 2004. Impact of freshwater input and wind on landings of anchovy (Engraulis encrasicolus) and sardine (Sardina pilchardus) in shelf waters surrounding the Ebre River delta (North Western Mediterranean). Fish. Oceanogr. 13 (2), 102–110.

Lötze, H.K., Coll, M., Dunne, J., 2011. Historical changes in marine resources, food-web structure and ecosystem functioning in the Adriatic Sea. Ecosystems 14, 198–222. https://doi.org/10.1007/s10021-010-9404-8.

Marrec, P., Grégori, G., Doglioli, A.M., Dugenne, M., Della Penna, A., Bhairy, N., Cariou, T., Hélias Nunige, S., Lahbib, S., Rougier, G., Wagener, T., Thyssen, M., 2018. Coupling physics and biogeochemistry thanks to high-resolution observations of the phytoplankton community structure in the northwestern Mediterranean Sea. Biogeosciences 15 (5), 1579–1606. https://doi.org/10.5194/bg-15-1579-2018.

Marty, J.-C., Chiavérini, J., Pizay, M.-D., Avril, B., 2002. Seasonal and interannual dynamics of nutrients and phytoplankton pigments in the western Mediterranean Sea at the DYFAMED time-series station (1991–1999). Deep Sea Res. II 49, 1965–1985. https://doi.org/10.1016/S0967-0645(02)00022-X.

Mayot, N., D'Ortenzio, F., Ribera d'Alcalà, M., Lavigne, H., Claustre, H., 2016. Interannual variability of the Mediterranean trophic regimes from ocean color satellites. Biogeosciences 13, 1901–1917. https://doi.org/10.5194/bg-13-1901-2016.

Mayot, N., D'Ortenzio, F., Uitz, J., Gentili, B., Ras, J., Vellucci, V., Golbol, M., Antoine, D., Claustre, H., 2017. Influence of the phytoplankton community structure on the spring and annual primary Production in the Northwestern Mediterranean Sea. J. Geophys. Res. Oceans 122, 9918–9936. https://doi.org/10.1002/2016JC012668.

McGillicuddy, D.J., 2016. Mechanisms of physical-biological-biogeochemical interaction at the oceanic mesoscale. Annu. Rev. Mar. Sci. 8, 125–159. https://doi.org/10.1146/annurev-marine-010814-015606.

MEDOC Group, 1970. Observations of formation of deep-water in the Mediterranean Sea. Nature 227, 1037–1040.

Mora, C., Frazier, A.G., Longman, R.J., Dacks, R.S., Walton, M.M., Tong, E.J., Sanchez, J.J., Kaiser, L.R., Stender, Y.O., Anderson, J.M., Ambrosino, C.M., Fernandez-Silva, I., Giuseffi, L.M., Giambelluca, T.W., 2013. The projected timing of climate departure from recent variability. Nature 502, 183–187. https://doi.org/10.1038/nature12540.

Morfin, M., Fromentin, J.-M., Jadaud, A., Bez, N., 2012. Spatio-temporal patterns of key exploited marine species in the Northwestern Mediterranean Sea. PLoS One 7 (5), e37907https://doi.org/10.1371/journal.pone.0037907.

Moutin, T., Thingstad, T.F., Van Wambeke, F., Marie, D., Slawyk, G., Raimbault, P., Claustre, H., 2002. Does competition for nanomolar phosphate supply explain the predominance of the cyanobacterium Synechococcus?. Limnol. Oceanogr. 47 (5), 1562–1567. https://doi.org/10.4319/lo.2002.47.5.1562.

Oliveros-Ramos, R., Shin, Y.J., 2016. Calibrar: a R Package for Fitting Complex Ecological Models. arXiv:1603.03141. 15 pp..

Palomera, I., Olivar, M.P., Salat, J., Sabatés, A., Coll, M., Garcia, A., Morales-Nin, B., 2007. Small pelagic fish in the NW Mediterranean Sea: an ecological review. Prog. Oceanogr. 74, 377–396. https://doi.org/10.1016/j.pocean.2007.04.012378.

Piroddi, C., Coll, M., Liquete, C., Macias, D., Greer, K., Buszowski, J., Steenbeek, J., Danovaro, R., Christensen, V., 2017. Historical changes of the Mediterranean Sea ecosystem: modelling the role and impact of primary productivity and fisheries changes over time. Sci. Rep. 7, 44491. https://doi.org/10.1038/srep44491.

Rigual-Hernandez, A.S., Barcena, M.A., Jordan, R.W., Sierro, F.J., Flores, J.A., Meier, K.J.S., Beaufort, L., Heussner, S., 2013. Diatom fluxes in the NW Mediterranean: evidence from a 12-year sediment trap record and surficial sediments. J. Plankton Res. 35 (5), 1109–1125. https://doi.org/10.1093/plankt/fbt055.

Rose, K., 2012. End-to-end models for marine ecosystems: are we on the precipice of a significant advance or just putting lipstick on a pig?. Sci. Mar. 76 (1), 195–201. https://doi.org/10.3989/scimar.03574.20B.

Sacchi, J., 2008. Impact des techniques de pêche sur l'environnement en Méditerranée. GFCM Stud. Rev. 84, 1–82.

San Feliu, J.M., Munoz, F., 1971. Fluctuations d'une année à l'autre dans l'intensité de l'affleurement dans la Méditerranée occidentale. Invest. Pesq. 35 (1), 155–159.

Saraux, C., Fromentin, J.-M., Bigot, J.-L., Bourdeix, J.-H., Morfin, M., Roos, D., et al., 2014. Spatial structure and distribution of small pelagic fish in the Northwestern Mediterranean Sea. PLoS One 9 (11), e111211https://doi.org/10.1371/journal.pone.0111211.

Saraux, C., Van Beveren, E., Brosset, P., Queiros, Q., Bourdeix, J.-H., Dutto, G., Gasset, E., Jac, C., Bonhommeau, S., Fromentin, J.-M., 2018. Small pelagic fish dynamics: a review of mechanisms in the Gulf of Lions. Deep-Sea Res. II: Top. Stud. Oceanogr. https://doi.org/10.1016/j.dsr2.2018.02.010.

Severin, T., Conan, P., Durrieu de Madron, X., Houpert, L., Oliver, M.J., Oriol, L., Caparros, J., Ghiglione, J.F., Pujo-Pay, M., 2014. Impact of open-ocean convection on nutrients, phytoplankton biomass and activity. Deep Sea Res. I 94, 62–71. https://doi.org/10.1016/j.dsr.2014.07.015.

Shin, Y.-J., Cury, P., 2004. Using an individual-based model of fish assemblages to study the response of size spectra to changes in fishing. Can. J. Fish. Aquat. Sci. 61, 414–431. https://doi.org/10.1139/f03-154.

Shin, Y.-J., Travers, M., Maury, O., 2010. Coupling low and high trophic levels models: towards a pathways-orientated approach for end-to-end models. Prog. Oceanogr. 84 (1-2), 105–112. https://doi.org/10.1016/j.pocean.2009.09.012.

Siokou-Frangou, I., Christaki, U., Mazzocchi, M.G., Montresor, M., Ribera d'Alcalà, M., Vaqué, D., Zingone, A., 2010. Plankton in the open Mediterranean Sea: a review. Biogeosciences 1586, 1543–1586. https://doi.org/10.5194/bg-7-1543-2010.

Somot, S., Houpert, L., Sevault, F., Testor, P., Bosse, A., Taupier-Letage, I., Bouin, M.-N., Waldman, R., Cassou, C., Sanchez-Gomez, E., Durrieu de Madron, X., Adloff, F., Nabat, P., Herrmann, M., 2018. Characterizing, modelling and understanding the climate variability of the deep water formation in the North-Western Mediterranean Sea. Clim. Dyn. 51 (3), 1179–1210. https://doi.org/10.1007/s00382-016-3295-0.

Travers-Trolet, M., Shin, Y.-J., Jennings, S., Machu, E., Huggett, J.A., Field, J.G., Cury, P.M., 2009. Two-ways coupling versus one-way forcing of plankton and fish models to predict ecosystem changes in the Benguela. Ecol. Modell. 220, 3089–3099. https://doi.org/10.1016/j.ecolmodel.2009.08.016.

Travers-Trolet, M., Shin, Y.-J., Shannon, L.J., Moloney, C.L., Field, J.G., 2014. Combined fishing and climate forcing in the Southern Benguela upwelling ecosystem: an end-to-End modelling approach reveals dampened effects. PLoS One 9, e94286https://doi.org/10.1371/journal.pone.0094286.

The MerMex Group, Durrieu de Madron, X., Guieu, C., Sempéré, R., Conan, P., Cossa, D., D'Ortenzio, F., Estournel, C., Gazeau, F., Rabouille, C., Stemmann, L., et al., 2011. Marine ecosystems' responses to climatic and anthropogenic forcings in the Mediterranean. Prog. Oceanogr. 91 (2), 97–166. https://doi.org/10.1007/978-1-4020-6772-3_3.

Ulses, C., Estournel, C., Bonnin, J., Durrieu de Madron, X., Marsaleix, P., 2008. Impact of storms and dense water cascading on shelf-slope exchanges in the Gulf of Lions (NW Mediterranean Sea). J. Geophys. Res. 113, C02010https://doi.org/10.1016/j.csr.2008.01.015.

Ulses, C., Auger, P.-A., Soetaert, K., Marsaleix, P., Diaz, F., Coppola, L., Herrmann, M.J., Kessouri, F., Estournel, C., 2016. Budget of organic carbon in the north-western Mediterranean Open Sea over the period 2004-2008 using 3-D coupled physical-biogeochemical modeling. J. Geophys. Res. Oceans 121, 7026–7055. https://doi.org/10.1002/2016JC011818.

Van Beveren, E., Bonhommeau, S., Fromentin, J.M., Bigot, J.L., Bourdeix, J.H., Brosset, P., Roos, D., Saraux, C., 2014. Rapid changes in growth, condition, size and age of small pelagic fish in the Mediterranean. Mar. Biol. 161, 1809–1822. https://doi.org/10.1007/s00227-014-2463-1.

Van Beveren, E., Fromentin, J.M., Bonhommeau, S., Nieblas, A.E., Metral, L., Brisset, B., Jusup, M., Klaus Bauer, R., Brosset, P., Saraux, C., 2017. Predator–prey interactions in the face of management regulations: changes in Mediterranean small pelagic species are not due to increased tuna predation. Can. J. Fish. Aquat. Sci. 74 (9), 1422–1430. https://doi.org/10.1139/cjfas-2016-0152.

Volpe, G., Nardelli, B.B., Cipollini, P., Santoleri, R., Robinson, I.S., 2012. Seasonal to interannual phytoplankton response to physical processes in the Mediterranean Sea from satellite observations. Remote Sens. Environ. 117, 223–235. https://doi.org/10.1016/j.rse.2011.09.020.